

Stability and quasinormal modes for black holes with time-dependent scalar hair

Sergi Sirera^{1,2} and Johannes Noller^{2,1}

¹*Institute of Cosmology & Gravitation, University of Portsmouth, Portsmouth, PO1 3FX, U.K.*

²*Department of Physics & Astronomy, University College London, London, WC1E 6BT, U.K.*

(Dated: August 6, 2024)

We investigate black hole solutions with time-dependent (scalar) hair in scalar-tensor theories. Known exact solutions exist for such theories at the background level, where the metric takes on a standard GR form (e.g. Schwarzschild-de Sitter), but these solutions are generically plagued by instabilities. Recently, a new such solution was identified in [1], in which the time-dependent scalar background profile is qualitatively different from previous known exact solutions - specifically, the canonical kinetic term for the background scalar X is not constant in this solution. We investigate the stability of this new solution by analysing odd parity perturbations, identifying a bound placed by stability and the resulting surviving parameter space. We extract the quasinormal mode spectrum predicted by the theory, finding a generic positive shift of quasinormal mode frequencies and damping times compared to GR. We forecast constraints on these shifts (and the single effective parameter $\hat{\beta}$ controlling them) from current and future gravitational wave experiments, finding constraints at up to the $\mathcal{O}(10^{-2})$ and $\mathcal{O}(10^{-6})$ level for LVK and LISA/TianQin, respectively. All calculations performed in this paper are reproducible via a companion Mathematica notebook [2].

CONTENTS

I. Introduction	1
II. Scalar-tensor theories and hairy black holes	2
III. Background stability and perturbations	3
A. Cosmological background	4
B. Black hole background	5
C. Perturbations	5
D. Stability conditions	7
IV. Quasinormal modes	8
A. Modified Regge-Wheeler equation	8
B. Quasinormal frequencies	9
V. Forecasted constraints	12
VI. Conclusions	13
Acknowledgments	14
A. Hairy black hole solutions	14
1. Static scalar	14
2. Time-dependent scalar	14
a. Existence of solutions	14
b. Stability	15
B. Background equations of motion	15
C. Large- r effects on QNMs	17
1. Metric background	17
2. Scalar background	17
References	18

I. INTRODUCTION

Ringdown tests of gravity: The rise of gravitational wave science offers a new way to probe gravity in the strong field regime. In particular, the final stage of gravitational wave signals emitted by binary compact object mergers, known as the ringdown, can be notably sensitive to new gravitational physics. The ringdown phase is well modelled by linear perturbations on a black hole background, whose evolution is described by a superposition of complex decaying frequencies, or quasinormal modes (QNMs) [3]. General Relativity (GR) predicts that the full set of QNMs is fixed by the black hole's mass and angular momentum (and charge, if present). This is a consequence of no-hair theorems in GR [4], and is therefore generically violated in extensions of GR which allow for hairy solutions. In such cases, QNMs can depend on extra parameters associated with the hair, and so looking for deviations from the GR-predicted QNM spectrum provides a powerful null test of GR. More quantitatively, QNM measurements can therefore be used to place constraints on (additional) fundamental gravitational degrees of freedom generically associated with extensions of GR that leave an imprint on the QNM spectrum [5]. This program, sometimes referred to as testing the *Kerr hypothesis*¹, or *black hole spectroscopy* [7], has been employed to probe the strong gravity regime in a diverse number of ways, see e.g. [8–24].

Black hole-scalar solutions: In this paper we will work in the context of scalar tensor theories, more specifically Horndeski (scalar-tensor) gravity [25, 26], which is the most general theory built with a metric tensor and a scalar field yielding second-order equations of motion. Black hole solutions to such theories broadly divide into two categories. On one hand,

¹ Formally, the Kerr hypothesis asks whether the final stage after gravitational collapse is well described by the Kerr geometry, and therefore contains no hair [6].

we have *stealth* black hole solutions, where the background metric takes the same form as known GR solution such as Schwarzschild or Schwarzschild-de Sitter (SdS). Any potential ‘hair’ associated to such stealth solutions is then associated only with the profile of the background scalar. On the other hand, due to the increased complexity of scalar tensor actions with respect to the Einstein-Hilbert action, more general black hole solutions can also exist in such theories. Thus, the other category of black hole solutions involve new background solutions for the metric itself (as well as for the scalar) – see e.g. [27, 28]. In this paper, we focus on the former, i.e. stealth black hole solutions with non-trivial scalar profiles. In particular, we will focus on Schwarzschild and SdS black hole solutions. Especially SdS solutions have been a focus of attention in previous studies [1, 29–39], since the de Sitter asymptotics at large distances more closely mimic realistic black holes embedded in cosmological space-times (in comparison to Schwarzschild solutions with their Minkowski asymptotics). In section II we will recap S(dS) solutions found in scalar-tensor theories, where the scalar has a time-dependent profile. But looking ahead, known exact solutions 1) generically suffer from instabilities, and 2) have been investigated for scalar profiles where $X \equiv -\frac{1}{2}\phi_\mu\phi^\mu$, the kinetic term for the scalar ϕ , is constant.

In this paper we therefore focus on a novel black hole solution that was recently found within Horndeski scalar-tensor theories [1] and is a promising candidate going beyond the constant X assumption and possibly providing stable dynamics as well. This theory is given by the following Lagrangian

$$\mathcal{L} = 2\eta\sqrt{X} - 2\Lambda + R(1 + \lambda\sqrt{X}) + \frac{\lambda}{2\sqrt{X}} [(\square\phi)^2 - \phi^{\mu\nu}\phi_{\mu\nu}], \quad (1)$$

where one can see that standard GR plus a decoupled scalar (albeit with non-standard kinetic term) is recovered in the $\lambda \rightarrow 0$ limit. This theory possesses an exact background solution of the form [1]

$$ds^2 = -B(r)dt^2 + \frac{1}{B(r)}dr^2 + d\Omega^2, \quad (2)$$

$$\bar{\phi} = qt + \psi(r),$$

with

$$B(r) = 1 - \frac{2M}{r} - \frac{1}{3}\Lambda r^2. \quad (3)$$

The background solution for the metric is therefore manifestly of SdS form and q is a (dimensionful) constant characterising the linear time-dependence of the scalar field, with ψ encoding its radial dependence. As we are dealing with a shift symmetric theory, the derivatives of the scalar field encode its most important features. In particular, the radial derivative of the scalar field and the kinetic term X are given by

$$\psi'^2 = \frac{q^2}{B^2} \left(1 - \frac{\lambda B}{\lambda + \eta r^2} \right), \quad (4)$$

$$X = \frac{1}{2} \frac{q^2 \lambda}{\lambda + \eta r^2},$$

where it is immediately apparent that this is a scalar profile with non-constant X and we illustrate the dependence of X on r in Figure 1. Our focus in this paper will therefore be to investigate this novel solution further, specifically its stability and QNM spectrum.

Outline: The paper is organised as follows. In section II we recap relevant hairy black hole solutions – in particular stealth black hole SdS solutions with linearly time-dependent scalar profiles – discovered so far and discuss related stability issues. In section III we examine the main theory of interest for this paper (1) at the background and perturbative level. We investigate the behaviour of linear odd parity perturbations on the hairy black hole background (2) and show when such perturbations are stable. In section IV we derive the corresponding modified Regge-Wheeler equation and employ the WKB method to extract the associated QNM spectrum. Finally, in section V we forecast constraints on the parameter that controls deviations from GR via a Fisher information analysis, before concluding in section VI and collecting further relevant details in the appendices. Throughout we work in *geometric* units, where $c = \hbar = G = 1$, unless explicitly stated otherwise.

II. SCALAR-TENSOR THEORIES AND HAIRY BLACK HOLES

In this section we briefly review the current state of hairy black hole solutions and their known stability properties. Our focus is on theories where the new fundamental physics is characterised by a single scalar degree of freedom ϕ , thus constituting a scalar-tensor theory. As previously noted, Horndeski gravity is the most general such theory resulting in second-order equations of motion [25, 26]², and is governed by the following action

$$S = \int d^4x \sqrt{-g} \left[G_2 + G_3 \square\phi + G_4 R + G_{4X} [(\square\phi)^2 - \phi^{\mu\nu}\phi_{\mu\nu}] + G_5 G_{\mu\nu} \phi^{\mu\nu} - \frac{1}{6} G_{5X} [(\square\phi)^3 - 3\phi^{\mu\nu}\phi_{\mu\nu}\square\phi + 2\phi_{\mu\nu}\phi^{\mu\sigma}\phi_\sigma^\nu] \right]. \quad (5)$$

Here we have introduced the short-hands $\phi_\mu \equiv \nabla_\mu \phi$ and $\phi_{\mu\nu} \equiv \nabla_\nu \nabla_\mu \phi$, the G_i are free functions of ϕ and X , where we recall that $X \equiv -\frac{1}{2}\phi_\mu\phi^\mu$, and \square is the d’Alembert operator. When discussing previous work on black hole solutions in scalar tensor theories, we will occasionally also refer to solutions derived in extensions of Horndeski theories, in particular within DHOST [41–45].

Horndeski gravity admits a richer variety of black hole solutions compared to GR. Yet, akin to GR, there exist a number of no-hair theorems for a wide range of scalar-tensor theories

² For the equivalence between the formulations of [25] and [26], see [40].

which enforce the scalar to possess a trivial profile [46–49].³ Stealth black holes with a constant scalar field background profile $\bar{\phi}$ have therefore been investigated in [11, 12, 50]. Around this background odd metric perturbations trivially behave just as in GR, since they are unaffected by the even sector (where scalar perturbations do induce non-trivial effects) and also do not feel any effects from the scalar background solution (since this is trivial in the present no-hair setup). Consequently, in order to explore potentially observable effects induced by the scalar, one ought to either investigate different background solutions (and hence consider Horndeski theories that evade no-hair theorems) or consider even perturbations. For detailed discussions of the second option we refer to [11, 12, 51–59] for work in the context of Horndeski gravity, and to [5, 52, 60–64] for work in the context of other theories (scalar-tensor or otherwise). However, here we will proceed along the first route, considering the dynamics of odd perturbations around background solutions which evade no-hair theorems. There exist a number of loopholes around no-hair theorems and one can broadly classify the constructed hairy solutions depending on whether the background scalar is static or contains a (typically linear) time-dependence. We summarise in Appendix A the existence of static radial hair solutions, but focus here exclusively on subsets of Horndeski which admit stealth black hole metrics with a time-dependent scalar as a background solution as in (2) of Schwarzschild or Schwarzschild-de Sitter (SdS) form

$$\begin{aligned} B &= 1 - \frac{2M}{r}, & \text{Schwarzschild,} \\ B &= 1 - \frac{2M}{r} - \frac{1}{3}\Lambda r^2, & \text{SdS.} \end{aligned} \quad (6)$$

Here M is the mass of a spherically symmetric compact object (e.g. a black hole) and Λ is a cosmological constant. Note that since we are focusing on stealth solutions where $B(r)$ is given by a GR metric, the scalar hair introduced by q is of secondary nature.⁴

Solutions of the form of (2) have been found to be of special cosmological interest, where the time-dependent scalar can affect cosmological dynamics and e.g. play the role of dark energy. More generally speaking, when embedding black hole solutions in a cosmological spacetime time-diffeomorphisms are naturally broken in the long-distance limit (unlike for Schwarzschild solutions with Minkowski asymptotics) and hence a time-dependent solution for the scalar is a natural occurrence in such settings. Calculating and measuring physical effects arising from such a time-dependence on the gravitational waves emitted by black holes therefore promises to

provide informative constraints on models such as (1). In this work we will focus on the imprints left on the quasinormal modes in the ringdown signal of binary black hole mergers by the non-trivial nature of the scalar field. However, a key requirement that needs to be satisfied prior to carrying out a ringdown study is for the solution to be stable, i.e. to avoid an unphysical (exponential) growth of perturbations. And indeed, while SdS solutions (i.e. approximants to "cosmological black hole" solutions) have been found for several sections of the Horndeski family, they have also been generically found to suffer from instabilities when the scalar has a time-dependent profile. Table I summarises the existence and stability of these types of solutions, and we provide in Appendix A a more in-depth and historical examination of the results collected there. Here, it suffices to say that, while such exact SdS and scalar profile solutions have been found for large subclasses of Horndeski theories, higher- ℓ even modes around backgrounds of the form of (2) have been shown to generically suffer from instability or strong coupling issues [60].

This then leaves us with no known well-behaved stealth black hole solutions with a linearly time-dependent scalar. However, as pointed out above, $X = \text{const}$ is a key requirement for the results of [60] to hold, so an obvious question is whether solutions with different scalar profiles exist and, if so, whether perturbations can be stable on such other backgrounds where $X \neq \text{const}$.⁵ While previous solutions have frequently been constructed by first imposing $X = \text{const}$ for simplicity (see e.g. a related discussion in [35]) and then finding the form of ψ satisfying this condition, the theory (1) was recently identified as possessing a stealth SdS solution for which $X \neq \text{const}$ [1]. In terms of Horndeski functions, this theory is given by

$$G_2 = -2\Lambda + 2\eta\sqrt{X}, \quad G_4 = 1 + \lambda\sqrt{X}, \quad G_3 = 0 = G_5. \quad (7)$$

As pointed out above, unlike previous solutions, X then adopts a non-trivial radial profile, cf. equations (2) and (4). In the next section we will therefore examine this theory at the background and perturbative level, showing that the solution can be stable under odd parity perturbations, and showing the effects on its (likewise odd parity) quasinormal mode spectrum.

III. BACKGROUND STABILITY AND PERTURBATIONS

Re-expressing (7) as a full action for the theory, we have

$$S = \int d^4x \sqrt{-g} \left[R \left(1 + \lambda\sqrt{X} \right) - 2\Lambda + 2\eta\sqrt{X} \right]$$

³ This was first shown for stationary black holes in minimally coupled Brans-Dicke theories [46], and subsequently extended to a more general class of scalar-tensor theories including self-interactions of the scalar [47], to spherically symmetric static black holes in Galilean-invariant theories [48], and for slowly rotating black holes in more general shift-symmetric theories [49].

⁴ Non-stealth solutions with primary hair have also been found in [1], but we will not be considering here.

⁵ Note that an alternative route to bypass stability issues in specific theories and to study the evolution of perturbations in a model-independent way (detached from the question of whether a given perturbative solution can be embedded in a full covariant theory) is to employ an Effective Field Theory (EFT) formalism to perturbations on a background with a time-dependent scalar. Such formalism has been developed recently in [67] and employed in different scenarios [21, 68–71]. In this work, however, we will focus on model-specific exact black hole solutions. In the context of realising well-behaved perturbative setups within covariant theories, also see work on the ‘scordatura mechanism’ [72, 73].

\mathcal{L}	Background solution		Stability	
	$g_{\mu\nu}$	X	odd	even
(Shift + refl)-sym Horndeski [29, 30]	S(dS)*	$\frac{q^2}{2} = \text{const}$	✓	✗
Cubic Galileon [31, 32]	S(dS)* (non-exact)	non-const (non-exact)	?	?
Shift-sym breaking Horndeski [65]	\ddagger (for large subclasses)	\ddagger (for large subclasses)	-	-
$G_2 = \eta X$, $G_4 = \zeta + \beta\sqrt{X}$ [33]	S(dS)* + RN(dS)* (non-exact)	non-const	?	?
Shift-sym beyond Horndeski [34]	SdS*	$\frac{q^2}{2} = \text{const}$	✓	✗
Shift-sym breaking quadratic DHOST [35]	S(dS)*	$\frac{q^2}{2} = \text{const}$	✓	✗
Shift-sym quadratic DHOST [36, 66]	S(dS)* + K*	const	✓	✗
Quadratic DHOST [37]	S(dS)* + (K)RN(dS)*	const	✓	✗
$G_2 = -2\Lambda + 2\eta\sqrt{X}$, $G_4 = 1 + \lambda\sqrt{X}$ [1]	S(dS)	$\frac{1}{2} \frac{q^2\lambda}{\lambda + \eta r^2}$	✓(this work)	?

TABLE I. Stealth black hole solutions with a linearly time-dependent scalar (2). S(dS) corresponds to Schwarzschild(-de Sitter), while (K)RN(dS) refers to (Kerr-)Reissner-Nordsröm(-de Sitter). The cosmological constant in dS can either come from a bare cosmological constant in the action as in GR, or from an effective combination of beyond-GR parameters (i.e. self-tuned). We denote cases which can fall in the latter category with *. The symbol \ddagger is used to indicate the non-existence of stealth black hole solutions – in particular such solutions were shown to be absent in large classes of shift symmetry breaking Horndeski theories in [65]. Further details related to all the solutions shown in this table are discussed in Appendix A. Let us only point out here that even modes have been shown to suffer from instabilities in all known hairy solutions for which $X = \text{const}$ [60]. This table builds on a pre-existing one [36].

$$+ \frac{\lambda}{2\sqrt{X}} \left((\square\phi)^2 - (\phi_{\mu\nu})^2 \right), \quad (8)$$

where the second line comes from the G_{4X} term. It is worth making explicit that, just as for the metric determinant, the square root of X is taken to be the principal (positive) square root. Upon a redefinition of the scalar field one can absorb into the scalar field either of the two parameters η or λ and hence redefine the theory without loss of generality in terms of only one parameter. This will be important when investigating and constraining physical deviations from GR in sections IV and V. In particular, we will redefine the scalar field as $\phi \rightarrow \frac{\phi}{\eta}$ and use $\beta^2 \equiv \frac{\lambda}{2\eta}$ as the single parameter controlling (small) departures from GR. In this section, in order to facilitate comparison with [1], we will however keep both η and λ as bookkeeping parameters. We collect in appendix B expressions for the covariant equations of motion, the current associated with the theory's shift-symmetry (demonstrating its regularity), and show a relation between the scalar and metric equations.

A. Cosmological background

We will focus on black hole solutions and related perturbations in this paper and hence primarily investigate (8) as a fiducial effective description of physics on the corresponding scales. Nevertheless, given the Schwarzschild-de Sitter stealth solution for the metric, it is interesting to briefly discuss the long-distance, ‘cosmological’ de Sitter limit of the dynamics encoded in (8). Focusing on the background evolution in the cosmological $r_s/r \ll 1$ limit, one can map the de Sitter metric in spherically symmetric coordinates – the long distance limit of (6) – to standard cosmological coordinates by using the transformations [31]

$$t = \tau - \frac{1}{2H} \ln \left[1 - (He^{H\tau}\rho)^2 \right]$$

$$r = e^{H\tau}\rho, \quad (9)$$

where $\Lambda = 3H^2$. This transformation then yields the metric

$$ds^2 = -d\tau^2 + e^{2H\tau}(d\rho^2 + \rho^2 d\Omega^2), \quad (10)$$

up to corrections $\mathcal{O}(r_s/r)$, i.e. terms strongly suppressed in the cosmological long distance limit. The Hubble parameter H is a constant in the de Sitter limit we are considering here. In these new coordinates, the canonical scalar kinetic term X is given by

$$X = \frac{1}{2} \frac{q^2\lambda}{\lambda + e^{2\sqrt{\frac{\Lambda}{3}}\tau}\eta\rho^2} = \frac{e^{-2\sqrt{\frac{\Lambda}{3}}\tau}q^2\lambda}{2\eta\rho^2} + \mathcal{O}\left(\frac{1}{\rho^4}\right), \quad (11)$$

where we again see that X is asymptotically suppressed at large distances. The fact that the effective cosmological constant is Λ (i.e. is not redressed by contributions from the scalar) as well as (11) serve to highlight two key points: 1) In the solution we are considering, the scalar field ϕ does not affect the cosmological background solution and e.g. is therefore not playing the role of dark energy. While, as discussed above, time-dependent scalar hair is often motivated by the way in which this time-dependence can be linked to cosmological background dynamics, this is therefore not a primary motivation for the specific solution we investigate here. 2) The form of X (11) and the fact that it is asymptotically suppressed at large distances means that this is not a solution where one obtains *both* $\phi \propto \tau$ in cosmological coordinates *and* a metric solution of the simple cosmological form (10). Instead, a significant (unsuppressed) ρ -dependence remains present in the ϕ profile.

Having briefly considered the background evolution, especially in the context of perturbative dynamics it is interesting to note that the theory we are investigating (7) belongs to the class of ‘extended cuscuton’ theories [74] – also see [75, 76]

for the original cuscuton theory. These theories satisfy the following condition

$$\mathcal{G}_T \mathcal{K} + 6\mathcal{M}^2 = 0, \quad (12)$$

where $\mathcal{G}_T, \mathcal{K}, \mathcal{M}$ are defined for general Horndeski theories in [74], but specialised to our setup are given by

$$\begin{aligned} \mathcal{G}_T &= 2(G_4 - 2XG_{4X}), & \mathcal{M} &= 2H\partial_\tau\phi(G_{4X} + 2XG_{4XX}), \\ \mathcal{K} &= G_{2X} + 2XG_{2XX} + 6H^2(G_{4X} + 8XG_{4XX} + 4X^2G_{4XXX}). \end{aligned} \quad (13)$$

It is straightforward to check that (7) satisfies $\mathcal{K} = 0$ and $\mathcal{M} = 0$, hence trivially meeting the condition (12). For such theories, [74] show that the scalar manifestly does not propagate when expressed in coordinates such that $\phi \propto \tau$. While we do not work in a coordinate system where $\phi \propto \tau$ here, the timelike nature of the derivative of ϕ means a transformation to new coordinates \tilde{x}^μ such that $\phi \propto \tilde{\tau}$ is expected to exist. Note that the metric is likewise expected to take on a form different from (10) in this new coordinate system. While we will not investigate the cosmological limit in different coordinate systems or further detail here, it will be interesting to investigate the link to cosmological cuscuton analyses further in the future. In the same vein it will also be interesting to in the future go beyond the odd parity perturbations around black hole backgrounds we focus on here. Investigating the even parity sector of (7) will in particular allow an assessment of whether scalar perturbations (which are even parity and hence do not show up in the odd sector) propagate in the black hole solutions considered here and precisely how this connects to the cosmological limit at large distances.⁶

B. Black hole background

Having briefly discussed cosmological limits, let us now move to the black hole backgrounds which are the main focus of this paper. We recall from equations (3) and (4) that it was shown in [1] that the theory (1) has a solution of the form (2) with⁷

$$\begin{aligned} B(r) &= 1 - \frac{2M}{r} - \frac{\Lambda r^2}{3}, \\ \psi'^2 &= \frac{q^2}{B^2} \left(1 - \frac{\lambda B}{\lambda + \eta r^2} \right), \end{aligned} \quad (14)$$

where the scalar kinetic term is consequently given by

$$X = \frac{q^2}{2B} - \frac{1}{2}B\psi'^2 = \frac{1}{2} \frac{q^2\lambda}{\lambda + \eta r^2}. \quad (15)$$

⁶ For a related study of black hole perturbations on a cuscuton-like model see [77], where it is found that in their set up odd parity modes evolve in the same way as in GR. Related to cosmological dynamics, while the model investigated here does not alter the cosmological expansion and dark energy is just given by a cosmological constant, we note that other cuscuton-related models can affect dark energy dynamics [78].

⁷ We refer to our reproducible Mathematica notebook for the details [2].

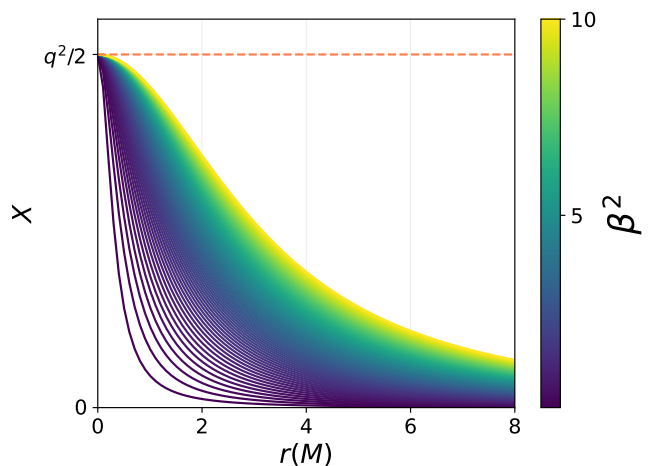


FIG. 1. Here we plot X (15), the standard kinetic term for the background scalar as a function of r . We show different choices for β , defined as $\beta^2 = \frac{\lambda}{2\eta}$. Smooth continuous lines exist only for $\beta^2 > 0$, i.e. η and λ having the same sign. In fact, it will be shown in section III D that $\beta^2 > 0$ is necessary to guarantee stability for all r . The horizontal orange dashed line at $X = q^2/2$ corresponds to the limit $\eta = 0$.

As mentioned above, unlike for other known time-dependent solutions, the kinetic term X here is not a constant but rather contains a specific r -dependence (see Figure 1). Note that the presence of *both* η and λ is required in order to have $X \neq \text{const}$. The form of ψ in (14) ensures that both (B6) and (B7) are satisfied and thereupon guarantees the existence of stealth black hole solutions such as SdS.

C. Perturbations

In order to investigate the linear stability of the solution (14) in the theory (8) and extract the quasinormal spectrum we need to study the evolution of linear perturbations. Around the static and spherically symmetric backgrounds considered here such perturbations can be decomposed into odd and even parity perturbations (under rotations), which decouple from one another at linear order (i.e. they evolve independently from one another and can therefore be treated separately). We will work to leading (linear) order in this paper, but note that this decoupling does not hold at higher orders – see [79–84] for details on the behaviour of higher order modes. This linear order decoupling enables us to study the odd sector in isolation. Perturbations on the scalar are purely of even parity and therefore will not be considered here. Odd perturbations are however affected by the background solution they are propagating on, so odd metric perturbations will nevertheless be sensitive to the new physics encoded by the (background solution of the) scalar field ϕ . We split the full metric into background + perturbations as

$$g_{\mu\nu} = \bar{g}_{\mu\nu} + h_{\mu\nu}, \quad (16)$$

where $\bar{g}_{\mu\nu}$ is given by (2) and (14), and $h_{\mu\nu}$ are small perturbations on top of it. As we are considering the odd sector and hence no scalar perturbations will be present in our analysis, we will (in an abuse of notation) use the same symbol for the scalar field ϕ and its background value. In the Regge-Wheeler gauge [85], these look like

$$h_{\mu\nu}^{\text{odd}} = \begin{pmatrix} 0 & 0 & 0 & h_0 \\ 0 & 0 & 0 & h_1 \\ 0 & 0 & 0 & 0 \\ h_0 & h_1 & 0 & 0 \end{pmatrix} \sin\theta \partial_\theta Y_{\ell m}, \quad (17)$$

where we have set $m = 0$ without loss of generality as a consequence of the background metric being static. h_0 and h_1 are functions of (r, t) , where the t -dependence will be taken to be of the form $e^{-i\omega t}$.

To obtain the evolution of such linear perturbations, we need to work at quadratic order in the perturbed action

$$S^{(2)} = \frac{1}{2} \int d^4x \sqrt{-g} \left[\mathcal{L}_{GR}^{(2)} + \mathcal{L}_\eta^{(2)} + \mathcal{L}_\lambda^{(2)} \right], \quad (18)$$

where the expressions for the corresponding quadratic lagrangians are⁸

$$\mathcal{L}_{GR}^{(2)} = \frac{1}{2} (\nabla^\sigma h^{\mu\nu} (2\nabla_\nu h_{\mu\sigma} - \nabla_\sigma h_{\mu\nu}) + 2\Lambda h_{\mu\nu} h^{\mu\nu}), \quad (20)$$

$$\mathcal{L}_\eta^{(2)} = \frac{-\eta}{\sqrt{X}} (X h_{\mu\nu} h^{\mu\nu} + \phi^\mu \phi^\nu h_\mu^\sigma h_{\nu\sigma}), \quad (21)$$

$$\begin{aligned} \mathcal{L}_\lambda^{(2)} = \frac{-\lambda}{2\sqrt{X}} & \left[\nabla_\sigma h_{\mu\nu} \left(X (\nabla^\sigma h^{\mu\nu} - 2\nabla^\nu h^{\mu\sigma}) + \phi^\sigma \phi^\rho \left(\frac{1}{2} \nabla_\rho h^{\mu\nu} - 2\nabla^\nu h_\rho^\mu \right) + \phi^\mu \phi^\nu \nabla_\rho h^{\sigma\rho} + 2\phi^\mu \phi^\rho \nabla^\nu h_\rho^\sigma \right) \right. \\ & + h_{\mu\nu} \left(\frac{1}{2} h^{\mu\nu} ((\square\phi)^2 - \phi_{\rho\gamma} \phi^{\rho\gamma}) + 4h_\sigma^\nu (\Lambda \phi^\mu \phi^\sigma - \phi^{\sigma\mu} \square\phi + \phi_\rho^\mu \phi^{\rho\sigma}) + 4h_{\sigma\rho} \phi^\mu [\phi^\sigma]^\nu{}^\rho \right. \\ & + \frac{1}{2X} \left(h_\sigma^\nu \phi^\mu \phi^\sigma (\phi_{\rho\gamma} \phi^{\rho\gamma} - (\square\phi)^2) + 2\phi^{\sigma\rho} (\phi^\mu \phi^\nu \phi_{\{\sigma}^\lambda h_{\rho\}\lambda} - h_{\sigma\rho} \phi^\mu \phi^\nu \square\phi) \right) \\ & + 4\phi^\rho \phi^{\mu\sigma} (2\nabla_{[\sigma} h_{\rho]}^\nu + \nabla^\nu h_{\rho\sigma}) + 2\phi^\mu \phi^{\sigma\rho} (2\nabla_\sigma h_\rho^\nu - \nabla^\nu h_{\sigma\rho}) + 2\phi^\mu \phi^\nu \nabla_\rho h_\sigma^\rho \\ & + 2\phi^\sigma \phi_\sigma^\mu \nabla_\rho h^{\nu\rho} + 2\phi^\sigma \phi_{\sigma\rho} \nabla^{[\nu} h^{\rho]\mu} + 2\square\phi (\phi^\sigma \nabla_\sigma h^{\mu\nu} - 2\phi^\mu \nabla_\sigma h^{\nu\sigma} - 2\phi^\sigma \nabla^\nu h_\sigma^\mu) \\ & \left. \left. + \frac{1}{2X} \phi^\mu \phi^\nu \phi^\sigma (\phi_\sigma^\rho \nabla_\gamma h_\rho^\gamma + \phi^{\rho\gamma} (2\nabla_{[\rho} h_{\gamma]\sigma} - \nabla_\sigma h_{\rho\gamma})) \right] \right], \quad (22) \end{aligned}$$

Here, we have used the fact that some terms vanish for odd perturbations. e.g. the trace $h \equiv h_\mu^\mu = 0$ as can be seen from (17).⁹ We have used the metric equations of motion for this background, i.e. $R_{\mu\nu} = \Lambda g_{\mu\nu}$ and $R = 4\Lambda$, and the notation for symmetric and antisymmetric tensors as shown in Appendix B13. From the form of the quadratic action we can already make the following observations: (20) describes how odd parity modes propagate in GR, (21) provides modification to the effective potential only while (22) also provides modifications to the kinetic term.

Substituting the components (17) and the solution for the background scalar (2) and (14) into the quadratic action (18), integrating over the angular coordinates and performing several integrations by parts, we can write the action in the fol-

lowing form:

$$S^{(2)} = \int dt dr \left[a_1 h_0^2 + a_2 h_1^2 + a_3 \left(\dot{h}_1^2 + h_0^2 - 2\dot{h}_1 h_0' + \frac{4}{r} \dot{h}_1 h_0 \right) + a_4 h_0 h_1 \right], \quad (23)$$

where a dot and a prime denote derivatives with respect to t and r , respectively, and we have dropped an overall multiplicative factor of $2\pi/(2\ell+1)$ coming from angular integration. The a -coefficients are given by

$$\begin{aligned} a_1 &= \frac{\ell(\ell+1)}{r^2} \left[(r\mathcal{H})' + \frac{(\ell-1)(\ell+2)\mathcal{F}}{2B} \right], \\ a_2 &= -\frac{\ell(\ell+1)(\ell-1)(\ell+2)}{2} \frac{B}{r^2} \mathcal{G}, \\ a_3 &= \frac{\ell(\ell+1)}{2} \mathcal{H}, \\ a_4 &= \frac{\ell(\ell+1)(\ell-1)(\ell+2)}{r^2} \mathcal{I}. \quad (24) \end{aligned}$$

where the a_i are to be evaluated on the background. Expressions for $\{\mathcal{F}, \mathcal{G}, \mathcal{H}, \mathcal{I}\}$ are given by

$$\mathcal{F} = 2 \left(G_4 - \frac{q^2}{B} G_{4X} \right),$$

⁸ Note that here we use the standard definition of symmetric and antisymmetric tensors

$$A_{\{\mu\nu\}} \equiv \frac{1}{2}(A_{\mu\nu} + A_{\nu\mu}), \quad A_{[\mu\nu]} \equiv \frac{1}{2}(A_{\mu\nu} - A_{\nu\mu}). \quad (19)$$

⁹ Note that this is not true for even parity perturbations - we refer to [2] for full details and recall that we are working in Regge-Wheeler gauge here.

$$\begin{aligned} \mathcal{G} &= 2 \left(G_4 + \left(\frac{q^2}{B} - 2X \right) G_{4X} \right), \\ \mathcal{H} &= 2(G_4 - 2XG_{4X}), \\ \mathcal{J} &= 2q\Psi'G_{4X}, \end{aligned} \quad (25)$$

$$= -2 \left(r^2 \left(\frac{b_2}{r^3} \right)' + \mathcal{H} \right). \quad (33)$$

where in our case the G -functions take the form given by (7) but the formula applies to more general theories [86, 87]. Note that $\mathcal{J} \neq 0$ only due to the presence of the scalar hair $q \neq 0$. The quadratic action (23) contains two fields (h_0, h_1) , but describes only one dynamical degree of freedom. As shown in [87], the action can be rewritten to make this manifest.

$$S^{(2)} = \frac{\ell(\ell+1)}{4(\ell-1)(\ell+2)} \int dt dr \left[b_1 \dot{Q}^2 - b_2 Q'^2 + b_3 \dot{Q} Q' - (\ell(\ell+1)b_4 + V_{\text{eff}}(r))Q^2 \right], \quad (26)$$

where the new variable Q can be written in terms of the old ones as

$$Q = h_1 - h'_0 + \frac{2}{r}h_0 \quad (27)$$

and the b -coefficients are given by

$$\begin{aligned} b_1 &= \frac{\mathcal{F}\mathcal{H}^2 r^2}{B\mathcal{F}\mathcal{G} + B\mathcal{J}^2}, \\ b_2 &= \frac{B\mathcal{G}\mathcal{H}^2 r^2}{\mathcal{F}\mathcal{G} + \mathcal{J}^2}, \\ b_3 &= \frac{2\mathcal{H}^2 \mathcal{J} r^2}{\mathcal{F}\mathcal{G} + \mathcal{J}^2}, \\ b_4 &= \mathcal{H}. \end{aligned} \quad (28)$$

Note the presence of the cross term b_3 which includes one time and one radial derivative. By performing a time redefinition as described in [86, 88]

$$\tilde{t} = t + \int \frac{b_3}{2b_2} dr, \quad (29)$$

we can diagonalise the kinetic part of the Lagrangian and rewrite the quadratic action in the standard form

$$S^{(2)} = \frac{\ell(\ell+1)}{4(\ell-1)(\ell+2)} \int dt dr \left[\tilde{b}_1 (\partial_{\tilde{t}} Q)^2 - b_2 Q'^2 - (\ell(\ell+1)b_4 + V_{\text{eff}}(r))Q^2 \right], \quad (30)$$

with

$$\tilde{b}_1 = b_1 - \frac{b_3^2}{4b_2} = \frac{\mathcal{H}^2 r^2}{B\mathcal{G}}. \quad (31)$$

The potential is given by

$$V_{\text{eff}}(r) = r^2 \mathcal{H} \left(b_2 \left(\frac{1}{r^2 \mathcal{H}} \right)' \right) - 2\mathcal{H}. \quad (32)$$

where the second equation is obtained using the fact that $\mathcal{H} = 2$ in this theory and thus $\mathcal{H}' = 0$.

D. Stability conditions

Having written the quadratic action in the form of (26), we can easily identify the following conditions in order for perturbations to be well-behaved and not grow over the background

$$\tilde{b}_1 > 0, \quad b_2 \geq 0, \quad b_4 \geq 0. \quad (34)$$

Since $b_4 = \mathcal{H} = 2$, the last inequality, which ensures the avoidance of tachyonic instabilities, is always satisfied. Before analysing the first two conditions, it is important to show that they indeed are legitimate measures of stability. As was shown in [89], the Hamiltonian density in the (t, r) coordinates, i.e. as obtained from (26), might be unbounded from below. However, Hamiltonian densities are coordinate-dependent quantities, and by performing a time coordinate transformation of the type (29) and showing the boundedness from below of the Hamiltonian in the new (\tilde{t}, r) coordinates, which is also encapsulated by conditions (34), it suffices to guarantee stability [89]. In our background of interest, \tilde{b}_1 and b_2 take the form

$$\begin{aligned} \tilde{b}_1 &= 2r^2 \frac{1}{\frac{|q|}{\sqrt{2}} \sqrt{\lambda^2 + \eta \lambda r^2} + B(r)} > 0, \\ b_2 &= 2r^2 \frac{\frac{|q|}{\sqrt{2}} \sqrt{\lambda^2 + \eta \lambda r^2} + B(r)}{1 + \frac{|q|}{\sqrt{2}} \frac{\lambda^2}{\sqrt{\lambda^2 + \eta \lambda r^2}}} \geq 0. \end{aligned} \quad (35)$$

Note that $B(r)$ is a positive definite function of r , so to satisfy both inequalities and ensure the coefficients are real we require

$$\lambda^2 + \eta \lambda r^2 \geq 0. \quad (36)$$

Investigating this condition in the short and long distance limits and for a fiducial mass of $M = 1/2$, one finds

$$\begin{cases} \lambda^2 + \eta \lambda \geq 0 & \text{at } r = 2M, \\ \eta \lambda \geq 0 & \text{at } r \rightarrow \infty. \end{cases} \quad (37)$$

Note that the second condition is stronger than the first, meaning that $\eta \lambda \geq 0$ is a sufficient condition to guarantee stability for all r . It is instructive to point out that we have glossed over the difference between Schwarzschild and SdS metric backgrounds in deriving (37). In SdS it does not make sense to take $r \rightarrow \infty$, but instead there the cosmological horizon r_c serves as an appropriate long distance limit for r . However, $r_c \gg r_s$ by ~ 20 orders of magnitude, so corrections to (37) arising from this finite long-distance limit are very strongly suppressed and we can therefore work with (37) to very high accuracy even for SdS.

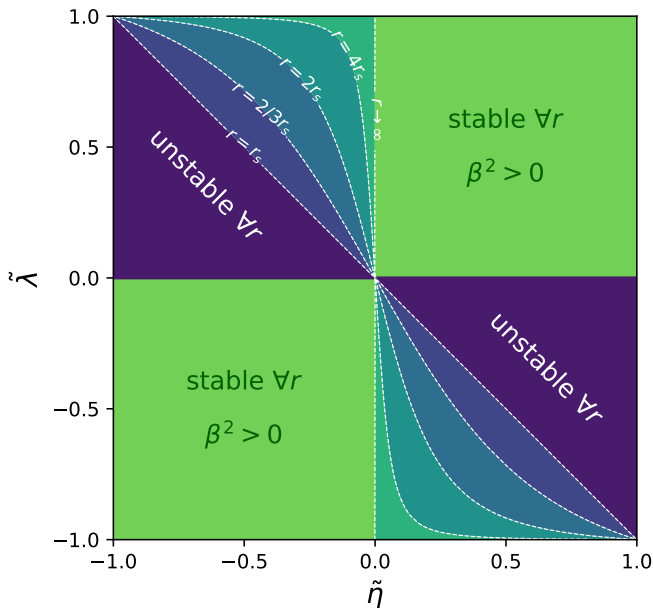


FIG. 2. Stability plot for black holes with a time-dependent scalar (2) in cuscuton-like theory (8). In the bright green region, stability is ensured for all r . At $r = r_s \equiv 2M$, the stable region is extended to cover up to the diagonal lines (37). In between the two extremes, there is a smooth r -dependent transition as shown by the dashed contours. Finally, the dark blue region corresponds to parameter values violating the stability conditions for all r . The plot we show here is a 2D representation of what really is a 3D space, where the extra dimension is given by r . In [2] we include an interactive 3D version of this plot which might help in its understanding.

To visualise the stability conditions in the full parameter space, we can compactify the infinite range of r as well as η and λ , i.e. $-\infty \leq (\gamma, \kappa) \leq \infty$ into a finite range. This can be done with the choices¹⁰

$$\tilde{\eta} = \frac{\eta}{\sqrt{1+\eta^2}}, \quad \tilde{\lambda} = \frac{\lambda}{\sqrt{1+\lambda^2}}. \quad (39)$$

Now, the full range of $\tilde{\eta}$ and $\tilde{\lambda}$ is given by $-1 \leq (\tilde{\eta}, \tilde{\lambda}) \leq 1$. Figure 2 summarises the results of our stability analysis using these variables.

As can be easily appreciated from the figure, stability conditions share certain symmetries in the η and λ plane. This is indeed not surprising, since (as discussed at the start of this section) one can rewrite the theory we consider in terms of only one free parameter, namely the ratio between λ and η . More specifically, we can redefine the scalar field $\phi \rightarrow \phi/\eta$,

¹⁰ Note that inverting this one gets

$$\eta \equiv \frac{\tilde{\eta}}{\sqrt{1-\tilde{\eta}^2}}, \quad \lambda \equiv \frac{\tilde{\lambda}}{\sqrt{1-\tilde{\lambda}^2}}. \quad (38)$$

which maps the action (8) to the following

$$S = \int d^4x \sqrt{-g} \left[M_{\text{Pl}}^2 R - 2\Lambda + 2M_{\text{Pl}}^2 \sqrt{X} + 2\beta^2 R \sqrt{X} + \frac{\beta^2}{\sqrt{X}} ((\square\phi)^2 - (\phi_{\mu\nu})^2) \right], \quad (40)$$

where we have temporarily suspended geometric units to make powers of M_{Pl} explicit and have implicitly defined the parameter β^2 as

$$\beta^2 \equiv \frac{\lambda}{2\eta} \geq 0, \quad (41)$$

where the final inequality is mandated by the stability conditions (37). Note that defining the parameter as β^2 is precisely motivated by those stability conditions, but the square root structure of the theory will mean several predictions in the following sections are controlled by $\beta \equiv \sqrt{\beta^2}$.

IV. QUASINORMAL MODES

Having set up the relevant perturbation theory and discussed stability properties in the previous section, we are now in a position to derive the corresponding quasinormal mode frequencies in the odd sector. As we will see, deviations from standard GR predictions will (as one may expect) be controlled by the β parameter introduced above.

A. Modified Regge-Wheeler equation

In order to obtain the analogue of the Regge-Wheeler equation we will follow the procedures described in [88]. We start by obtaining the equation of motion for the master variable Q of the odd parity perturbations by applying the variational principle to (26)

$$-\partial_t^2 Q + \frac{b_2}{\tilde{b}_1} Q'' + \frac{b_2'}{\tilde{b}_1} Q' - \frac{\ell(\ell+1)b_4 + V_{\text{eff}}}{\tilde{b}_1} Q = 0. \quad (42)$$

To remove the single radial derivative term, we express the equation above in a generalisation of the tortoise coordinate given by¹¹

$$r_* = \int \sqrt{\frac{\tilde{b}_1}{b_2}} dr \quad (43)$$

and redefine Q as

$$\Psi = FQ \quad (44)$$

where

$$F = (\tilde{b}_1 b_2)^{1/4}. \quad (45)$$

¹¹ Note that for $\lambda = 0$ we recover the tortoise coordinate in GR $dr_* = \frac{1}{b} dr$.

Doing this, we obtain an expression in the form of the Regge-Wheeler equation

$$(\partial_*^2 - \partial_{\tilde{r}}^2 - V)\Psi = 0, \quad (46)$$

where we have expressed the tortoise derivative as $\frac{\partial}{\partial r_*} \equiv \partial_*$.

$$V = V_{RW} \left(1 + \frac{q\beta\sqrt{2\beta^2 + r^2}}{B} \right) + \frac{q\beta(B + q\beta\sqrt{2\beta^2 + r^2})}{4r^2(2\beta^2 + r^2)(2q\beta^3 + \sqrt{2\beta^2 + r^2})^3} \times$$

$$\times \left[q^2\beta^6(192\beta^4 + 104\beta^2r^2 + 3r^4) + 2(2\beta^2 + r^2)(24\beta^4 + 17\beta^2r^2 + 2r^4) + 6q\beta^3\sqrt{2\beta^2 + r^2}(384\beta^4 + 416\beta^2r^2 + 117r^4) \right.$$

$$\left. - \beta^2B \left(2(48q^2\beta^6(2\beta^2 + r^2) + 48\beta^4 + 56\beta^2r^2 + 19r^4) \right) + \frac{q\beta^3}{\sqrt{2\beta^2 + r^2}}(384\beta^4 + 416\beta^2r^2 + 117r^4) \right]. \quad (48)$$

where V_{RW} is the well-known Regge-Wheeler potential in GR

$$V_{RW} = B \left(\frac{\ell(\ell+1)}{r^2} - \frac{6M}{r^3} \right), \quad (49)$$

and, as discussed above, square roots in (48) denote principal square roots (this is also the origin of odd powers of β seen in the potential).

In the next section we will investigate the quasinormal frequencies and damping times of this potential. There, we will find that, at leading order, deviations from GR are in fact controlled by a single effective parameter, namely

$$\hat{\beta} \equiv \beta \frac{Mq}{M_{\text{Pl}}^3}. \quad (50)$$

Let us now look at how the potential V looks analytically when $\hat{\beta} \ll 1$, so as to better understand its parametric form. To this end it is instructive to write the potential as

$$V = V_{RW} + \sum_{i=1} \delta V_i \times \hat{\beta}^i. \quad (51)$$

with the first orders of δV_i given by

$$\delta V_1 = \frac{1}{Mr} \left(M_{\text{Pl}}^2(\ell(\ell+1) + 1) - \frac{8M}{r} \right),$$

$$\delta V_2 = \frac{M_{\text{Pl}}^4}{M^2},$$

$$\delta V_3 = \frac{M_{\text{Pl}}^2}{q^2 M^3 r^3} \left(M_{\text{Pl}}^4(\ell(\ell+1) - 4) + \frac{21MM_{\text{Pl}}^2}{r} - \frac{38M^2}{r^2} \right),$$

$$\delta V_4 = \frac{M_{\text{Pl}}^6}{q^2 M^4 r^2} \left(\frac{56M}{r} - 15M_{\text{Pl}}^2 \right), \quad (52)$$

where we have again temporarily suspended geometric units to make powers of M_{Pl} (and hence mass dimensions) explicit. Higher orders can be found in the companion Mathematica

The potential is given by

$$V = \frac{\ell(\ell+1)b_4 + V_{\text{eff}}}{\tilde{b}_1} + \frac{1}{F} \partial_*^2 F. \quad (47)$$

and V_{eff} is given by (33). The full analytical expression for V can be written as

notebook [2]. The effect of δV on the unperturbed V_{RW} is shown in Figure 3, where one can appreciate almost a constant shift in the amplitude of the potential throughout the range of the radial coordinate.

B. Quasinormal frequencies

Having obtained the effective potential for the modified Regge-Wheeler equation, we can now study its quasinormal mode solutions. Looking for quasi-normal mode solutions where Ψ has a time dependence of $e^{-i\omega t}$, we can write the Regge-Wheeler equation as

$$(\partial_*^2 + \omega^2 - V)\Psi = 0. \quad (53)$$

Upon imposing the dissipative boundary conditions

$$\Psi \sim \begin{cases} e^{-i\omega r_*}, & \text{for } r_* \rightarrow -\infty, \\ e^{i\omega r_*}, & \text{for } r_* \rightarrow \infty, \end{cases} \quad (54)$$

which correspond to outgoing waves at spatial infinity and incoming waves at the black hole horizon, the ω solutions to (53) become complex and can therefore be written as

$$\omega_{\ell m} = 2\pi f_{\ell m} + \frac{i}{\tau_{\ell m}}. \quad (55)$$

Here, the real part corresponds to the physical oscillation frequency of a mode, while the imaginary part corresponds to its damping time. Due to the axisymmetric nature of our background modes with different (ℓ, m) indices do not mix.¹² Here we will mainly focus on the dominant mode $(2, 2)$.

¹² There is a third index characterising the QNM spectrum, the overtone number n . Here we only focus on the ‘fundamental mode’ $n = 0$. Modes with higher n 's (i.e. overtones) are more suppressed by virtue of having increasing values of $|\text{Im}(\omega)|$.

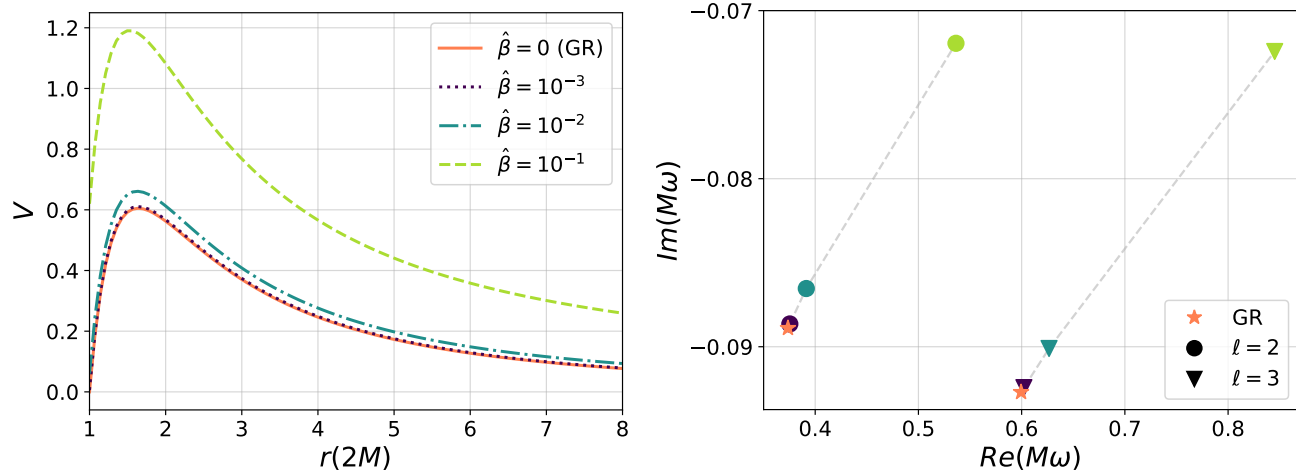


FIG. 3. **Left panel:** Modified Regge-Wheeler potential for different magnitudes of the deviation parameter $\hat{\beta}$ for $\ell = 2$. We show r in units of $r_s = 2M$, so that $r = 1$ corresponds to $r = r_s$. One can observe that the main effect is an enhancement in the overall amplitude. Also note that the maximum of the potential is slightly shifted to lower values of r . **Right panel:** Quasinormal modes for $\ell = 2$ (corresponding to table II) and $\ell = 3$ for increasing magnitudes of $\hat{\beta}$. Both stars correspond to the GR values and colours correspond to $\hat{\beta}$ values on the left panel.

There are a number of techniques one can use to obtain the QNM themselves (see e.g. [90–97]) but we refer to [3] for an extensive review of those. Here, we will use the WKB method, first applied to black holes in [92] and subsequently extended to higher orders in [98–101].¹³ We do this by adapting the Mathematica package which can be found in [101, 105].

The WKB method provides a straightforward and precise technique of obtaining quasinormal frequencies from an effective potential in a semi-analytical manner. However, in order for it to be justifiably applied, the potential needs to satisfy some criteria laid out in [101]. Most notably, the potential must have one local maximum, be asymptotically constant, and contain two turning points. As can be observed from Figure 3, these are all satisfied by our modified effective potential.¹⁴

Let us now briefly introduce how the method works practically. The rationale is to match the asymptotic solutions given by (54) respectively with a Taylor expansion around the maximum of the potential located at r_0 . For a differential equation written in the form of (53), the matching of solutions at the different regions imposes

$$\omega^2 = V_0 - i \left(n + \frac{1}{2} \right) \sqrt{2V_0^{(2)}} - i \sqrt{2V_0^{(2)}} \sum_{i=2}^N \Lambda_j. \quad (56)$$

¹³ Because of the form of the potential corrections (52), in particular the fact that they do not scale with $B(r)$, it is unfortunately challenging to use the parametrised ringdown formalism introduced in [97] and subsequently developed in [102–104].

¹⁴ Note that, as is also the case for the GR potential in 3, the second turning point for the modified potentials is hidden at $r < 1$, where V approaches $+\infty$ as $r \rightarrow 0$.

Here, V_0 denotes the potential evaluated at the maximum r_0 , and we use $V_0^{(2)}$ to denote the second tortoise derivative of V evaluated at the maximum. n , being the overtone number, is set to zero when focusing on the fundamental mode. Finally, Λ_j are functions of higher order derivatives of the potential, where j denotes the order to which the WKB expansion is carried out. The first application of this method to black holes was carried out in [92] and included only the first order. [98] then extended the WKB formula to 3rd order by computing Λ_2 and Λ_3 . This was then extended in [99] to 6th order and in [100] to 13th order. However, going up in WKB order does not necessarily mean improving accuracy. For instance, the fundamental mode in GR is best approximated by 6th order WKB [105], and we find that this is also true when including our corrections.¹⁵ Therefore, we perform calculations to 6th order WKB in what follows.

Note that obtaining QNMs via the WKB method involves taking derivatives at the maximum of the potential. The location of the maximum, however, changes as a function of $\hat{\beta}$. The WKB package [105] allows one to obtain numerical values for the QNMs while taking this into account automatically, and we show some examples in table II and figure 3 calculated this way.

Nonetheless, we also want ‘semi-analytical’ expressions for ω as a function of $\hat{\beta}$ that we can then use in our forecast analysis. For this, we employ the *light ring expansion* [53] to find the location of the maximum as a function of $\hat{\beta}$. The expansion works under the assumption that the geometry is

¹⁵ We show in [2] that this is the case by computing how error estimation increases with WKB order. As said, we find that this is minimised for 6th order.

	Re($M\omega$)	Im($M\omega$)
$\hat{\beta} = 0$ (GR)	0.3736	-0.0889
$\hat{\beta} = 10^{-3}$	0.3754	-0.0886
$\hat{\beta} = 10^{-2}$	0.3914	-0.0865
$\hat{\beta} = 10^{-1}$	0.5364	-0.0719

TABLE II. Real and imaginary components of the $\ell = 2$ quasinormal frequencies ω for varying $\hat{\beta}$ obtained with the WKB method to 6th order.

"quasi-Schwarzschild" or, in other words, that the location of the potential maximum is only a small deviation away from the Schwarzschild value $r_*^{\max} = r_*^{\max, \text{GR}} + \delta r_*$. This is certainly true in our case of study with small $\hat{\beta}$, as can be seen from figure 3.¹⁶ Upon employing the light ring expansion we can expand the defining property of the maximum of the potential $\delta_r V|_{r=r_*^{\max, \text{GR}} + \delta r_*} = 0$ to approximate to first order [53]

$$\delta r_* = - \frac{\partial_r V}{\partial_r^2 V} \Big|_{r=r_*^{\max, \text{GR}}} \quad (57)$$

With this, we then have expressions for the maximum as a function of $\hat{\beta}$ that we can then substitute in all the potential derivatives in (56). While the full expression of $r_*^{\max}(\hat{\beta})$ is quite lengthy – see [2] for full details – this simplifies considerably for small $\hat{\beta}$, i.e. the case we are focusing on here. But rather than immediately truncating to the lowest order correction in $\hat{\beta}$, it is instructive to examine the few lowest order terms. We find

$$\begin{aligned} \frac{M_{\text{Pl}}^2}{M} r_*^{\max} &= 3.2808 - 3.0306 \cdot \hat{\beta} + 0.8316 \cdot \hat{\beta}^2 \\ &- \left(0.22819 + 1.8502 \frac{M_{\text{Pl}}^8}{M^4 q^2} \right) \cdot \hat{\beta}^3 + \mathcal{O}(\hat{\beta}^4) \end{aligned} \quad (58)$$

where we have set $\ell = 2$ in deriving this expression, and the first term represents the GR value $r_*^{\max, \text{GR}} = 3.2808 \cdot M/M_{\text{Pl}}^2$. This expression highlights three important points:

1. First, the regime where it makes sense to truncate the above expansion is $\hat{\beta} \ll 1$. This corresponds to $\beta M q \ll M_{\text{Pl}}^3$, which puts an implicit bound on the (until now unrestricted) parameter q if we are to demand working in the small $\hat{\beta}$ regime, i.e. in the regime where potential deviations and the shift of r_*^{\max} are small. As an example, taking $\beta \sim \mathcal{O}(1)$ and considering black holes with $M \sim \mathcal{O}(10)M_\odot$, where $M_\odot \sim 10^{30}\text{kg}$ while $M_{\text{Pl}} \sim 10^{-8}\text{kg}$, this requirement becomes $\sqrt{q} \ll 10^{-28}\text{kg}$ or, equivalently, $\sqrt{q} \ll 10^8 \text{ eV}$.
2. At cubic order in $\hat{\beta}$ we effectively see that the theory ultimately is controlled by two parameters (in addition

to M and M_{Pl}): β and q . While at lower (leading) orders these only enter in the form of the single effective parameter $\hat{\beta}$, from cubic order onwards we can see q entering independently. Note that this is expected in light of the potential corrections (52), which share this feature. If we require these qualitatively different terms (e.g. the second term in the second line of (58)) to be suppressed with respect to the solely $\hat{\beta}$ -dependent terms, we in addition require $M_{\text{Pl}}^8 \ll M^4 q^2$. Taking the same example masses as above, this is akin to requiring $\sqrt{q} \gg 10^{-47} \text{ kg}$ or $\sqrt{q} \gg 10^{-11} \text{ eV}$. When this bound is satisfied, these additional terms can be safely dropped for black hole mass ranges close to the example chosen here.

3. For small $\hat{\beta}$, the linear $\hat{\beta}$ term in (58) is the leading order correction. An immediate consequence of this is that the maximum of the potential always decreases in such cases, getting closer to the light ring at $r = 3M$ compared to GR.

Equipped with (58), we can substitute this into the WKB formula (56) to obtain an expression for the QNM frequencies in terms of $\hat{\beta}$, i.e. $\omega(\hat{\beta})$. Since the full expression is quite cumbersome, we do not show it here (but leave it available in [2] for the interested reader). We have checked that the ω values found with this analytical expression agree with those in table II. Working in a small $\hat{\beta}$ expansion, one then finds

$$\begin{aligned} \frac{M\omega}{M_{\text{Pl}}^2} &= \frac{M\omega_0}{M_{\text{Pl}}^2} + (1.80 + 0.25i)\hat{\beta} \\ &- (2.24 + 1.57i)\hat{\beta}^2 + \mathcal{O}(\hat{\beta}^3), \end{aligned} \quad (59)$$

where ω_0 is the GR prediction, satisfying $M\omega_0/M_{\text{Pl}}^2 = (0.37 - 0.09i)$, and the other terms correspond to entries in III. More precise and extensive coefficients for this expansion are given in this table, with corrections to the QNM frequencies parametrised via

$$\omega_N = \omega_0 + \sum_{i=1}^{i=N} \delta\omega_i \hat{\beta}^i. \quad (60)$$

The numerical precision of this expansion is shown in figure 4 for increasing N .

i	$M\delta\omega_i$		$M\omega_i(\hat{\beta} = 10^{-1})$	
	Re	Im	Re	Im
0	/	/	0.3736	-0.0889
1	1.7981	0.2474	0.5534	-0.0642
2	-2.2441	-1.5708	0.5310	-0.0799
3	5.6825	11.2960	0.5367	-0.0686
4	-8.8312	-66.8072	0.5358	-0.0752
5	-112.1770	388.5760	0.5347	-0.0714
6	1619.7700	-2009.9100	0.5363	-0.0734
7	-15232.1000	8055.9700	0.5348	-0.0726

TABLE III. Real and imaginary components of the corrections to the $\ell = 2$ quasinormal frequencies ω .

¹⁶ Note that the maximum is approximately located around the light ring, which in Schwarzschild GR is at $r = 3M$. In figure 3, because $r_s = 1$ has been chosen, the three maxima appear around $r(2M) \approx 1.5$.

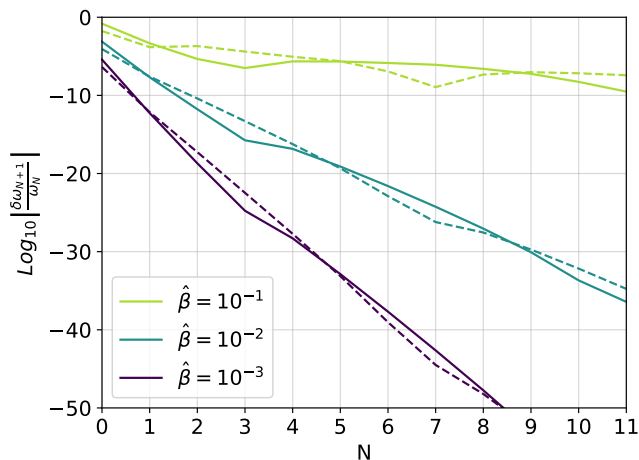


FIG. 4. This plot displays the achievable accuracy in the real (solid) and imaginary (dashed) parts of quasinormal modes for $\ell = 2$ for increasing orders of N in (60). The y-axis represents the fractional contribution to the quasinormal frequencies gained by going to the next $N + 1$ order as compared to ω_N . As can be seen, these fall off very quickly, resulting in $\mathcal{O}(10^{-6})$ corrections for $N \geq 7$ even for $\hat{\beta} \sim 0.1$.

V. FORECASTED CONSTRAINTS

In the previous section we obtained the QNM spectrum for a hairy black hole with a time-dependent scalar, where deviations from GR are controlled by the parameter $\hat{\beta}$, which encodes information about the underlying scalar-tensor theory. Our aim now is to forecast how well current and future GW experiments will be able to constrain $\hat{\beta}$ using solely the ringdown. Table IV collects our main results.

We employ a Fisher forecast analysis to estimate the precision with which $\hat{\beta}$ will be measurable. Our analysis ubiquitously uses techniques developed in [106] - for a detailed summary of the forecasting setup specialised to our present analysis see [8]. We will here focus on a simplified scenario where all the standard waveform parameters are already known (A, ϕ^+, \dots), leaving $\hat{\beta}$ as the only free parameter. Given this idealised setup, the constraints forecasted here should be interpreted as optimistic/optimal estimates for expected achievable precision. Forecasts with full joint constraints for all waveform parameters will be left for future work.

For a setup as considered here, where the only waveform parameters we want to constrain are those appearing inside the quasinormal frequencies ω , general expressions for the achievable precision can be derived analytically. These only depend on the number of parameters one wants to constrain. Here, GR deviations are solely controlled by the parameter $\hat{\beta}$ so we employ the expression for single-parameter constraints

$$\sigma_{\hat{\beta}}^2 \rho^2 = \frac{1}{2} \left(\frac{f}{Qf'} \right)^2, \quad (61)$$

where the prime denotes a derivative with respect to $\hat{\beta}$ - we refer to [8] for details on the derivation of (61). In (61), ρ refers to the standard signal-to-noise-ratio (SNR) and the quality factor Q is defined as

$$Q_{\ell m} = \pi f_{\ell m} \tau_{\ell m}. \quad (62)$$

In the context of astrophysical binary compact objects, the $(\ell, m) = (2, 2)$ mode is generically the one with largest amplitude and dominates the ringdown signal [106–111]. It is therefore usually referred to as the dominant mode. For non-rotating black holes, which are our focus here, the equations of motion do not depend on m [52]. Consequently, even though $m = 0$ is typically set for simplicity, as we have done here, the results are valid for any m . For discussions on the amplitude and detectability of subdominant modes we refer to [107, 109, 112, 113], but here highlight that not only does the $\ell = 2$ mode dominate in typical scenarios, but also note that for binary systems which have orbited each other sufficiently long, the orbits will have circularised, additionally enhancing the $\ell = 2$ mode relative to other modes [114–116]. That being said, our analysis here can straightforwardly be repeated for higher ℓ modes,¹⁷ while we leave conducting a multi-mode analysis and extending this study to slowly rotating black holes (see e.g. [118–122]) for future work. We can now use the semi-analytical expressions found for the $\hat{\beta}$ -dependent QNMs together with the error expression (61) to place estimated order-of-magnitude constraints on $\hat{\beta}$ and hence on the gravity model (1). Reading off f and Q from (60), as defined in (55) and (62), and substituting them into the single-parameter error expression (61), we obtain an estimate on its detectability in the same fashion as [8, 123].¹⁸ This gives us¹⁹

$$\sigma_{\hat{\beta}} \rho \approx 0.07. \quad (63)$$

The precision with which $\hat{\beta}$ can be constrained therefore inversely depends on the achievable SNR, which varies for different existing and upcoming detectors. Table IV collects updated estimates on the optimistic obtainable ringdown SNRs together with the corresponding order-of-magnitude constraint on $\hat{\beta}$ for several ground and space-based detectors. 3rd generation space based detectors such as LISA are predicted to be able to achieve a ringdown SNR as high as 10^5 , which would entail a constraint on $\hat{\beta}$ of

$$\sigma_{\hat{\beta}}^{\text{LISA/TianQin}} \sim 10^{-6}. \quad (64)$$

¹⁷ Note that the dipole mode $\ell = 1$ requires special treatment, as the Regge-Wheeler gauge does not completely fix the gauge in this case. For detailed information see [117], where it is also shown that $\ell = 1$ contributions are negligible in set ups as the one considered here.

¹⁸ Note that, in evaluating the final expression, we set $\hat{\beta}$ to zero. This should simply be understood as capturing the leading order contributions to the error - depending on the actual value of $\hat{\beta}$ the precise error can differ by $\lesssim \mathcal{O}(1\%)$ for $\hat{\beta} \lesssim 10^{-1}$.

¹⁹ A value with more significant figures is provided in [2]. Ultimately, we will approximate $\sigma_{\hat{\beta}} \rho \approx \mathcal{O}(10^{-1})$ in table IV, as we are purely interested in the robust order-of-magnitude constraints here.

Detector(s)	Ringdown SNR (ρ)	Error on $\hat{\beta}$
LVK	10 [132–134]	10^{-2}
ET / CE	10^2 [134–137]	10^{-3}
pre-DECIGO	10^2 [138]	10^{-3}
DECIGO / AEDGE	10^3 [139, 140]*	10^{-4}
LISA	10^5 [133, 141]	10^{-6}
TianQin	10^5 [141]	10^{-6}
AMIGO	10^5 [142]	10^{-6}

TABLE IV. Achievable order-of-magnitude ringdown SNRs for a single observed event for different GW detectors and the corresponding order-of-magnitude errors on $\hat{\beta}$. A star * denotes that the quoted forecasted SNR is not ringdown-specific. For ET/CE we have quoted the ringdown-specific ET forecast [134], in the current absence (to our knowledge) of an analogous forecast for CE. For LISA, we note that the quoted SNR is significantly larger than typical event SNRs in the LISA Mock Data Challenge which go up to $\sim \mathcal{O}(10^3)$ [143, 144], while [141] forecast SNRs up to $\sim \mathcal{O}(10^5)$ for sufficiently nearby and massive events. This also illustrates that there is still significant variance in the forecasted SNRs relevant for the missions considered here.

Let us stress here that the primary bounds discussed in this analysis are projected from a single ringdown observation with the SNR as described in Table IV. In fact, as the number of equivalent events N increases, such bounds are predicted to improve as $N^{1/2}$ [18, 124]. For the LISA band, this could entail an improvement in the constraint on $\hat{\beta}$ of up to two orders of magnitude, i.e. $\sigma_{\hat{\beta}}^{\text{LISA/TianQin}} \sim 10^{-8}$, as the estimated rates of SMBH mergers, despite somewhat uncertain, lie in the $\mathcal{O}(10 - 100)$ per year – see e.g. [3, 125–131].²⁰ Finally, let us point out that shifts in the QNM frequencies and damping times are detectable with approximately the same precision as constraints on $\hat{\beta}$, e.g. $\delta\omega \sim 10^{-6}$ will be detectable with LISA/TianQin. In our context this can e.g. be seen by noticing that the precision with which $\hat{\beta}$ is constrainable is inversely proportional to SNR (63), while the shift in QNM frequencies and damping times scales linearly with $\hat{\beta}$ (in the small $\hat{\beta}$ regime we are investigating) at leading order with order one coefficient(s) $\delta\omega_1 \sim 1.7981 + 0.2474i$.

VI. CONCLUSIONS

In this paper we have investigated the stability and quasinormal modes of odd parity perturbations of hairy black hole solutions with a linearly time-dependent scalar. In particular,

we have focused on the specific scalar-tensor theory identified in [1] and given by (1). This theory possesses an exact Schwarzschild-de Sitter solution for the metric ((4) and (2)) and the scalar field is indeed linearly time-dependent for this solution, but (unlike for other currently known exact solutions in scalar-tensor theories with these characteristics) the canonical scalar kinetic term $X \equiv -\frac{1}{2}\phi_\mu\phi^\mu$ is not constant. This solution is of particular interest since known constant X solutions are generically plagued by instabilities. Our key findings are:

- The solution we investigate can support stable odd parity perturbations, where a non-trivial bound on the theory’s coupling constant $\hat{\beta}^2 > 0$ is placed by requiring odd sector stability. This parameter is effectively a dimensionless measure of the strength of interactions in the theory (and suggestively written as $\hat{\beta}^2$, given this bound - note, however, that the square root structure of the theory means several theory predictions are controlled by $\hat{\beta} \equiv \sqrt{\hat{\beta}^2}$).
- We have derived the modified Regge Wheeler equation governing odd parity perturbations in this setup, and provided its quasinormal mode solutions. QNMs in this setting are controlled by the same single parameter $\hat{\beta}$ highlighted above. We have computed the QNM spectrum and quantified deviations from the GR values as a function of $\hat{\beta}$, finding the following qualitative features: 1) Both QNM frequencies and damping times are enhanced (i.e. have a positive-definite shift) when compared to GR in this theory, as illustrated in figure 3, 2) The maximum of the modified Regge-Wheeler potential shifts to smaller radii, lying closer to the light ring than in GR, 3) The overall amplitude of the modified Regge-Wheeler potential is enhanced (i.e. experiences a positive-definite shift, as above). The size of all three effects is controlled by $\hat{\beta}$.
- We derive forecasted constraints on $\hat{\beta}$ and the associated shifts in the quasinormal frequency spectrum for upcoming ringdown observations. A single LISA or TianQin event can constrain these shifts at (up to) the $\mathcal{O}(10^{-6})$ level, with the potential of improving this further by two orders of magnitude by stacking multiple events. In the regime of small shifts/small $\hat{\beta}$ we investigated, these shifts linearly depend on $\hat{\beta}$ and hence this parameter is constrainable at (up to) the $\mathcal{O}(10^{-6})$ level (plus potential improvements from stacking). A suitably loud LVK observations, on the other hand, can provide analogous constraints at (up to) the $\mathcal{O}(10^{-2})$ level. Table IV collects equivalent order-of-magnitude achievable constraints for several current and future detectors.

Several avenues therefore suggest themselves for future work extending the above: Most importantly, it will be interesting to see what complementary bounds the even sector will place and whether a fully stable corner of parameter

²⁰ This however assumes an optimistic scenario of N events with identical SNR, while many events will have lower SNR values, e.g. mergers at higher redshifts.

space remains for such theories when considering both odd and even parity perturbations. Considering the dynamics of the theory (1) in detail in other regimes, e.g. its cosmological dynamics/limit as briefly discussed here, promises to further constrain the relevant parameter space. More generally speaking, we hope this paper provides a stepping stone towards identifying the landscape of which (if any) black hole solutions with time-dependent scalar hair are fully stable and hence are of particular interest for both theoretical and observational follow-up investigations.

ACKNOWLEDGMENTS

We thank Eugeny Babichev and Kazufumi Takahashi for useful discussions. SS is supported by an STFC studentship. JN is supported by an STFC Ernest Rutherford Fellowship (ST/S004572/1). In deriving the results of this paper, we have used xAct [145] and [2].

Appendix A: Hairy black hole solutions

Hairy black hole solutions in scalar-tensor theories can broadly be divided in two categories, depending on whether the scalar is static or contains a linear time-dependence. We here briefly review both, concentrating more on the latter case, which is the focus of the present paper. They each violate no-hair theorems in different ways. In the context of shift-symmetric theories ($\phi \rightarrow \phi + c$), [146] proved that black holes cannot support non-trivial scalar profiles if the following assumptions apply²¹

1. The spacetime is spherically symmetric, static and asymptotically flat,
2. The scalar field is static $\phi(r)$ and has a vanishing derivative ϕ' at infinity,
3. The norm of the current associated with the shift-symmetry is finite down to the horizon,
4. The action contains a canonical kinetic term $X \subset G_2$,
5. All $G_i(X)$ functions are analytical at $X = 0$.

Time-dependent scalars automatically violate assumption 2, while static profiles will require the violation of an assumption other than 2. For reference, the hairy solution studied in the main text violates assumptions 2, 4 and 5.

²¹ A nice summary of the theorem and its consequences is provided in [147, 148], including this itemised list.

1. Static scalar

We begin by considering solutions where the metric and the scalar are both static and spherically symmetric

$$ds^2 = -B(r)dt^2 + \frac{1}{B(r)}dr^2 + d\Omega^2, \quad \bar{\phi} = \phi(r). \quad (\text{A1})$$

Arguably the most common and minimal setup to achieve such kind of radial scalar hair is via a linear coupling to the Gauss-Bonnet invariant [49, 149], given by the choices

$$G_2 = \eta X, \quad G_4 = \zeta, \quad G_5 = \alpha \ln |X|, \quad (\text{A2})$$

where η , ζ and α are constants and the other G_i 's are set to zero. The G_5 term is indeed equivalent to the linear coupling $\mathcal{L} \supseteq \alpha \phi \mathcal{G}$, where \mathcal{G} is the Gauss-Bonnet invariant [40].

There exist, however, more general ways of breaking assumptions in no-hair theorems and thus constructing hairy solutions of this kind. [33] showed that including at least one of the following

$$G_2 \supseteq \sqrt{X}, \quad G_3 \supseteq \ln |X|, \quad G_4 \supseteq \sqrt{X}, \quad G_5 \supseteq \ln |X|, \quad (\text{A3})$$

to an overall shift-symmetric action is sufficient to potentially enact a radial-dependent scalar profile. These additional operators are in principle of notable interest as, unlike in the scalar Gauss-Bonnet case, they result in a current with a finite norm at the horizon [33]. They do, however, come with potential issues, as it was shown that operators of the type (A3) other than the Gauss-Bonnet coupling lack a Lorentz invariant ($X = 0$) solution in Minkowski spacetime [150]. If such solutions are desired, this requirement can therefore be used to eliminate all solutions in (A3), except for the scalar-Gauss-Bonnet solution. Having said this, we note that the Lorentz-invariant $X = 0$ vacuum is also not a stable solution in Galileon cosmologies consistent with CMB constraints [151], so the absence of a healthy $X = 0$ solution need not imply the absence of relevant solutions in settings where Lorentz invariance is (already) spontaneously broken.

2. Time-dependent scalar

Let us now turn our attention to linearly time-dependent scalars, which directly violate assumption 2 and therefore require in principle no additional violations to generate hair. Table I provides a comprehensive summary of the discussion presented here.

a. Existence of solutions

They were firstly found in [29] for the theory given by

$$G_2 = -2\Lambda + 2\eta X, \quad G_4 = \zeta + \beta X, \quad (\text{A4})$$

with η , ζ and β being constants. The β -term introduces a non-minimal coupling of the scalar field to the Einstein tensor

(i.e. $\beta G^{\mu\nu} \phi_{,\mu} \phi_{,\nu}$)²² which has been referred to as the ‘John term’ in [152] and plays an essential role in driving expansion. This result was then generalised in [30] to the shift-symmetric ($\phi \rightarrow \phi + c$) and reflection-symmetric ($\phi \rightarrow -\phi$) Horndeski subset, of which (A4) is an example.²³ In particular, it is the shift symmetry of the scalar which allows it to possess a linear time-dependence while keeping the background metric static, as the background equations of motion will only depend on derivatives of ϕ [39].

As a specific case of (A3), [33] considered the theory given by

$$G_2 = \eta X, \quad G_4 = \zeta + \beta \sqrt{X} \quad (\text{A6})$$

and extended the construction of hairy black holes to the time-dependent background. The metric solution in this case was found to be non-stealth and hence we will not consider it here any further, but rather leave its stability analysis as a potential extension of this work.

It was also investigated in [31, 32] whether these time-dependent backgrounds could also be solutions of Horndeski theories incorporating G_3 such as the Cubic galileon, given by

$$G_2 = -2\Lambda\zeta + 2\eta X, \quad G_3 = -2\gamma X \quad G_4 = \zeta. \quad (\text{A7})$$

This choice breaks the reflection symmetry of the previously studied theories but keeps the shift symmetry. However, no exact stealth black hole solutions of the form of (2) were found. Instead, some approximated analytical expressions were given for different asymptotics, which we will not discuss here.

A breaking of shift-symmetry was also studied in [65], finding that solutions of the form (2) cannot exist there. This is no longer true, however, in beyond Horndeski theories, where such background configurations were found to be solutions of shift-symmetric [36, 37] and shift-symmetry breaking quadratic DHOST [35].

b. Stability

Despite being exact solutions to a considerably large class of scalar-tensor theories, backgrounds of the form of (2) were quickly shown to be prone to instability issues. Odd parity perturbations were initially argued in [87] to possess either ghost or gradient instabilities close to the black hole horizon. It was later pointed out in [89] that this statement, made on the

²² To check this, note that the β -term contributes to $G_{4X} = \beta$. One can then use the Ricci identity of commuting covariant derivatives alongside integration by parts to show that

$$G_{4X} [(\square\phi)^2 - \phi^{\mu\nu} \phi_{,\mu\nu}] = \beta R^{\mu\nu} \phi_{,\mu} \phi_{,\nu}. \quad (\text{A5})$$

Combining this with $G_4 R \ni -\beta \frac{1}{2} g^{\mu\nu} R \phi_{,\mu} \phi_{,\nu}$ gives us the coupling to the Einstein tensor.

²³ Other non-stealth black hole solutions were also found for this Horndeski subclass, but we will not be discussing them here.

unboundedness of the Hamiltonian density, was coordinate-dependent and therefore not a good stability criterion, which should be independent of coordinates.²⁴ In fact, it was shown there that stability could be attained in some time slicings for odd parity modes and even parity modes with $\ell = 0$. The assumption of reflection symmetry was dropped from the stability analysis in [153], thus including also the non-stealth solutions found in [32], and it was found that odd parity perturbations could be stable in some subclasses of shift-symmetric Horndeski. This analysis was then extended to the shift- and reflection-symmetric subclass of DHOST theories in [86], showing that odd parity perturbations there are stable and propagate with the same effective potential as in GR, i.e. the Regge-Wheeler potential.

However, higher- ℓ even modes for the same stealth solutions in DHOST were then investigated in [60], finding that they were unfortunately plagued with instability or strong coupling issues. In particular, it was found that even modes coming from scalar perturbations were always everywhere unstable (c.f. to just close to the horizon in [87]). This result was later confirmed in [38], which also found even gravitational modes to suffer from instabilities or be strongly coupled. This then leaves us with no known well-behaved stealth black hole solutions with a linearly time-dependent scalar. Being $X = \text{const}$ a key requirement for the results of [60] to hold, one can hope even parity perturbations might be stable in this configuration. We have shown in this paper that there exists an exact hairy black hole solution with non-constant X for which odd parity perturbations are stable.

In the context of non-exact stealth black hole solutions, which as mentioned before is not the focus of this paper, [154] looked at static solutions with a non-constant X and their stability against odd parity perturbations, finding that some configurations can be stable. When including time-dependence, however, no stable configuration was found.

Appendix B: Background equations of motion

Writing the Lagrangian (8) as

$$\mathcal{L} = \mathcal{L}_{GR} + \mathcal{L}_\eta + \mathcal{L}_\lambda, \quad (\text{B1})$$

with

$$\begin{aligned} \mathcal{L}_{GR} &= R - 2\Lambda, \\ \mathcal{L}_\eta &= 2\eta \sqrt{X}, \\ \mathcal{L}_\lambda &= \lambda \left(R\sqrt{X} + \frac{1}{2\sqrt{X}} ((\square\phi)^2 - (\phi_{,\mu\nu})^2) \right), \end{aligned} \quad (\text{B2})$$

the equations of motion from for the metric tensor and the scalar can respectively be written as

$$\mathcal{E}_{\mu\nu} = \mathcal{E}_{\mu\nu}^{GR} + \mathcal{E}_{\mu\nu}^\eta + \mathcal{E}_{\mu\nu}^\lambda = 0, \quad (\text{B3})$$

²⁴ We thank Eugeny Babichev for related discussions.

$$\mathcal{E}_\phi = \mathcal{E}_\phi^\eta + \mathcal{E}_\phi^\lambda = 0, \quad (\text{B4})$$

where we introduce the notation $\mathcal{E}_{\mu\nu}^i = \frac{\delta S_i}{\delta g^{\mu\nu}}$, $\mathcal{E}_\phi^i = \frac{\delta S_i}{\delta \phi}$, and we have used the fact that $\mathcal{E}_\phi^{GR} = 0$ since it is ϕ -independent. Full expressions for $\{\mathcal{E}_{\mu\nu}^{GR}, \mathcal{E}_{\mu\nu}^\eta, \mathcal{E}_{\mu\nu}^\lambda, \mathcal{E}_\phi^{GR}, \mathcal{E}_\phi^\eta, \mathcal{E}_\phi^\lambda\}$ are given below. We note that the above equations of motion satisfy an interesting relation given by

$$\nabla^\mu \mathcal{E}_{\mu\nu} = -\phi_{,\nu} \mathcal{E}_\phi. \quad (\text{B5})$$

This is in fact satisfied independently by the three different lagrangians in (B1). One can easily check from the expressions (B9) and (B12) that $\nabla^\mu \mathcal{E}_{\mu\nu}^\eta = -\phi_{,\nu} \mathcal{E}_\phi^\eta$. On the other hand, showing that $\nabla^\mu \mathcal{E}_{\mu\nu}^\lambda = -\phi_{,\nu} \mathcal{E}_\phi^\lambda$ is more cumbersome and is therefore shown in [2] for the interested reader. Then, one is

left with $\nabla^\mu \mathcal{E}_{\mu\nu}^{GR} = -\phi_{,\nu} \mathcal{E}_\phi^{GR}$. As was argued before, $\mathcal{E}_\phi^{GR} = 0$ due to the lack of ϕ -dependence, which in turn reassures that Bianchi identities are satisfied, i.e. $\nabla^\mu \mathcal{E}_{\mu\nu}^{GR} = 0$.

In this paper we are focusing on so-called ‘stealth’ solutions, where despite of dynamical modifications induced by the scalar field, the metric background solution is as it would be in standard GR (in our case: a standard SdS solution) and hence $\mathcal{E}_{\mu\nu}^{GR} = 0$. In that case equations (B3) and (B4) imply that the scalar background profile satisfies both

$$\mathcal{E}_{\mu\nu}^\eta = -\mathcal{E}_{\mu\nu}^\lambda, \quad (\text{B6})$$

$$\mathcal{E}_\phi^\eta = -\mathcal{E}_\phi^\lambda. \quad (\text{B7})$$

Here we give full expressions for $\{\mathcal{E}_{\mu\nu}^{GR}, \mathcal{E}_{\mu\nu}^\eta, \mathcal{E}_{\mu\nu}^\lambda, \mathcal{E}_\phi^{GR}, \mathcal{E}_\phi^\eta, \mathcal{E}_\phi^\lambda\}$

$$\mathcal{E}_{\mu\nu}^{GR} = R_{\mu\nu} - \frac{1}{2}g_{\mu\nu}(R - 2\Lambda), \quad (\text{B8})$$

$$\mathcal{E}_{\mu\nu}^\eta = -\frac{\eta}{\sqrt{X}} \left(Xg_{\mu\nu} + \frac{1}{2}\phi_{,\mu}\phi_{,\nu} \right), \quad (\text{B9})$$

$$\begin{aligned} \mathcal{E}_{\mu\nu}^\lambda = \frac{\lambda}{2\sqrt{X}} \left[-2X \left(R_{\mu\nu} - \frac{1}{2}g_{\mu\nu}R \right) + \frac{1}{2}\phi_{,\mu}\phi_{,\nu} \left(R - \frac{1}{2}(\square\phi)^2 \right) + \frac{1}{2}g_{\mu\nu} (2R_{\sigma\rho}\phi^\sigma\phi^\rho + \phi_{\sigma\rho}\phi^{\sigma\rho} - (\square\phi)^2) + \phi_{\mu\nu}\square\phi \right. \\ \left. - 2\phi^\sigma (\phi_{\{\mu}R_{\nu\}\sigma} + \phi_{\{\mu}\phi_{\nu\}\sigma}) - \phi_{\nu\sigma}\phi_{\mu}^\sigma - R_{\mu\sigma\nu\rho}\phi^\sigma\phi^\rho \right. \\ \left. + \frac{1}{2X} \left(2\phi^\sigma\phi_{\sigma\rho}\phi_{\{\mu}\phi_{\nu\}\rho} - \phi_{\mu\nu}\phi^\sigma\phi_{\rho\sigma}\phi^\rho - \frac{1}{2}\phi_{,\mu}\phi_{,\nu}\phi_{\sigma\rho}\phi^{\sigma\rho} + \phi_{\mu\sigma}\phi^\sigma\phi_{\nu\rho}\phi^\rho \right. \right. \\ \left. \left. + g_{\mu\nu}\phi^\sigma\phi^\rho (\square\phi\phi_{\sigma\rho} - \phi_{\rho\gamma} - \phi_{\rho\gamma}\phi_{\sigma}^\gamma) \right) \right], \quad (\text{B10}) \end{aligned}$$

$$\mathcal{E}_\phi^{GR} = 0, \quad (\text{B11})$$

$$\mathcal{E}_\phi^\eta = \frac{\eta}{\sqrt{X}} \left(\square\phi + \frac{1}{2X}\phi^\mu\phi^\nu\phi_{,\mu\nu} \right), \quad (\text{B12})$$

$$\begin{aligned} \mathcal{E}_\phi^\lambda = \frac{\lambda}{\sqrt{X}} \left[\frac{1}{2}R\square\phi - 2\phi_{,\mu\nu}\phi^{\mu\nu} + \square^2\phi - X\square\phi - R_{\mu\nu}\phi^\mu\phi^\nu - \frac{3}{2}\phi_{,\mu\nu}\phi^\mu\phi^\nu \right. \\ \left. + \frac{1}{2X} \left(-3\phi^\mu\phi^\nu\phi_{\mu\sigma}\phi_{\nu}^\sigma + \phi_{\sigma\nu} \left(-\phi^{\mu\nu}\phi_{\mu}^\sigma + \frac{1}{2}\square\phi\phi^{\sigma\nu} \right) + \phi^\mu \left(\frac{1}{2}R\phi^\nu\phi_{\mu\nu} - 2\phi_{\mu}^\nu\phi^\rho R_{\rho\nu} - \phi^\rho\phi_{\nu}^\sigma R_{\rho\sigma\mu} \right) \right) \right. \\ \left. + \frac{3}{(2X)^2}\phi^\mu\phi^\nu\phi_{\sigma\rho} \left(-\phi_{\mu}^\sigma\phi_{\nu}^\rho + \frac{1}{2}\phi_{\mu\nu}\phi^{\sigma\rho} \right) \right], \quad (\text{B13}) \end{aligned}$$

where we have used again the standard definition of symmetric and antisymmetric tensors (19).

As a consequence of the shift-symmetry of the theory considered here, the scalar equation of motion can be rewritten as a conservation equation

$$\mathcal{E}_\phi = -\nabla_\mu J^\mu = 0, \quad (\text{B14})$$

where the current J^μ can similarly be written as

$$J^\mu = J_\eta^\mu + J_\lambda^\mu \quad (\text{B15})$$

with [149]

$$J_\eta^\mu = -\frac{\eta}{\sqrt{X}}\phi^\mu, \quad (\text{B16})$$

$$\begin{aligned} J_\lambda^\mu = \frac{\lambda}{2\sqrt{X}} \left[G^{\mu\nu}\phi_{,\nu} - \frac{1}{2X} \left(\phi^\mu \left((\phi_{,\nu\sigma})^2 - (\square\phi)^2 \right) \right. \right. \\ \left. \left. + 2\phi^{\mu\nu} (\square\phi\phi_{,\nu} - \phi_{\nu\sigma}\phi^{\sigma\nu}) \right) \right]. \quad (\text{B17}) \end{aligned}$$

Note that $\mathcal{E}_\phi^\eta = -\nabla_\mu J_\eta^\mu$ and $\mathcal{E}_\phi^\lambda = -\nabla_\mu J_\lambda^\mu$. The norm of the current is given by

$$J^2 \equiv J_\mu J^\mu = \frac{1}{6r(\lambda + \eta r^2)} \left[384M\eta^2 - r(27\lambda^3\Lambda^2 + 108\eta^3 r^2 + 9\eta\lambda^2\Lambda(20 + 3\Lambda r^2) + 4\eta^2\lambda(75 + 29\Lambda r^2)) \right]. \quad (\text{B18})$$

Hence, the norm of the current is found to be regular for all r down to the black hole horizon.

Appendix C: Large- r effects on QNMs

Here we explore the effect that large r effects, i.e. features far away from the black hole, have on the emission of quasinormal modes. One would expect that such effects are strongly suppressed, as quasinormal mode emission should be governed by the local dynamics around the source. However, in the context of hairy black hole solutions in scalar-tensor theories one frequently (and unlike in the theory we focus on in this paper) does not know the exact scalar solution, but only approximate solutions accurate in the long- or short-distance limits. Quantifying the error one introduces in the predicted quasinormal mode spectrum by using an approximate solution can then be difficult. The known exact solution we investigate in this paper therefore provides an excellent testbed to quantify this error and we will investigate this by introducing by hand an ‘error’ (i.e. a deviation term) into the scalar field equation that only affects large distances, thus giving us a deformed scalar profile which is only a good approximation at short distances and hence mimicking the situation one encounters in other scalar-tensor theories. As a warm-up we first investigate the effect of a cosmological constant term (likewise a large- r effect) on the quasinormal mode spectrum along the lines investigated by [155, 156] and then consider the deformed scalar profile discussed above.

1. Metric background

First, we begin by considering the impact that terms which become important at large r in the background metric have on quasinormal frequencies. The formalism for this is already at hand, since that is precisely the nature of the Λ term in the SdS metric

$$B = 1 - \frac{2M}{r} - \frac{1}{3}\Lambda r^2. \quad (\text{C1})$$

Whether this really impacts at large r or not is of course dependent on the value of Λ . As was shown in [156], for cosmological values of Λ (i.e. $\Lambda/M_{\text{pl}}^2 = 10^{-52}\text{m}^{-2}$ in natural units) its effect on the QNMs is negligible. In particular, for a black hole of $10^6 M_\odot$, the correction to the quasinormal modes appears at the 10^{-34} level.

The SdS solution also allows for values of Λ bigger than the one for the cosmological constant. In particular, the range

of values owed for Λ which preserve the 2 horizon nature of SdS is $0 \leq \Lambda \leq \frac{1}{9M^2}$. QNM values spanning this full range of Λ were calculated in [155]. In the cases considered there, where the black hole and cosmological horizon are of comparable size it is not surprising that deviations in the frequencies become quite large.

We employ here the WKB method to obtain quasinormal frequencies in the two same ways as has been done in the main text. First, we apply the package [105] directly and obtain numerical solutions for specific values of Λ . By doing so, we find that our results agree well with [155]. Secondly, we use the 6th order WKB formula (56) and take derivatives of the potential while keeping Λ unspecified. Hence, we are able to obtain an expression for $\omega(\Lambda)$. As was the case with $\omega(\beta)$ in the main text, the expression is cumbersome and therefore unfeasible to write here. One can find such expression in [2]. Here, we instead Taylor expand around the zero value for Λ and obtain²⁵

$$M\omega = M\omega_0 - [1.67631 - 0.33463i] \cdot M^2\Lambda - [3.85847 - 0.89970i] \cdot M^4\Lambda^2 - [17.4684 - 6.04082i] \cdot M^6\Lambda^3 + \mathcal{O}(\Lambda^4). \quad (\text{C2})$$

where we recover $M\omega_0$ as the Schwarzschild quasinormal frequencies. Using this semi-analytical expressions, we are also able to recover the same results as in [155], gaining precision for smaller Λ . This also serves to test this semi-analytical prescription, which is used in the main text to constrain β .²⁶ Finally, for a black hole of $10^6 M_\odot \simeq 10^9 \text{m}$ ²⁷ and a cosmological constant of $\Lambda = 10^{-52} \text{m}^{-2}$, we can easily use equation (C2) to confirm that the first correction to the quasinormal frequencies appears at the 10^{-34} level, in agreement with [156].

2. Scalar background

Secondly, we also want to show that quasinormal modes are largely unaffected by large r modifications to the scalar background solution. We do so by introducing by hand into (4) an ‘error’ term that becomes important at some large scale

²⁵ Higher order contributions can be obtained in [2].

²⁶ The maximum of the potential is shifted due to Λ . Employing the *light-ring expansion* [53], for small values of Λ , this is given by

$$r_*^{\text{max}} = 3.28 \cdot M - 2.85 \cdot M^3 \Lambda + \mathcal{O}(\Lambda^2), \quad (\text{C3})$$

²⁷ Note the the mass of the Sun in geometric units is around $1.5\text{km} \simeq 10^3 \text{m}$.

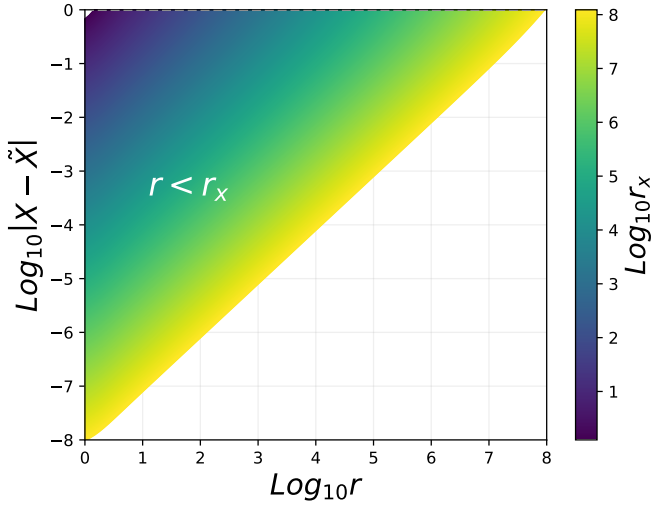


FIG. 5. Effect of the large- r term on the kinetic term X for a given r_x as a function of r . In line with the context in which we introduce the r_x correction (as a large r correction that only becomes $\mathcal{O}(1)$ at large scales), we only show the $r < r_x$ region. Indeed one can see how r_x -induced corrections to the scalar kinetic term are suppressed when $r \ll r_x$.

r_x as²⁸

$$\tilde{\psi}' = \frac{q}{B} \sqrt{1 - \frac{\lambda B}{\lambda + \eta r^2}} + q\lambda \left(\frac{r}{r_x}\right)^n \quad (\text{C5})$$

As generality is not our main focus here, we will show results for $n = 1$, which should in principle have larger contributions than higher n choices. Nonetheless, one could easily adapt the code in [2] for different n , and likewise for more general parametrisations of the large- r correction, such as making it not λ -dependent.

This extra term only becomes relevant at $r \gtrsim r_x$. To visualise this, we plot in Figure 5 the difference in the kinetic term with (\tilde{X}) and without (X) the large- r contribution, where one can see that $\tilde{X} \simeq X$ for $r \lesssim r_x$.

Using this background solution, we follow the equivalent steps as described in the text and we obtain modified potential correction coefficients to the ones in eq. (52). As a concrete example, the first two modified potential correction terms are

$$\delta\tilde{V}_1 = \frac{M_{\text{Pl}}^2 r ((\ell(\ell+1) + 1)r_x - (2\ell(\ell+1) + 5)M_{\text{Pl}}^2 r^3) - M(8r_x - 22M_{\text{Pl}}^2 r^3)}{M \frac{r^2}{\sqrt{r_x}} (r_x - 2M_{\text{Pl}}^2 r^3)^{3/2}}, \quad \delta\tilde{V}_2 = \frac{M_{\text{Pl}}^4 r_x (r_x - 5M_{\text{Pl}}^2 r^3)}{M^2 (r_x - 2M_{\text{Pl}}^2 r^3)^2}, \quad (\text{C6})$$

where we have again temporarily suspended geometric units to make powers of M_{Pl} (and hence mass dimensions) explicit. We can now neatly relate this back to the potential corrections found in eq. (52), i.e. in the absence of the scalar profile deviation introduced in (C5). Zooming in on the leading order contribution δV_1 , we can rewrite it as

$$\delta\tilde{V}_1 = \delta V_1 + M_{\text{Pl}}^2 \left[\frac{M_{\text{Pl}}^2 r}{M} (\ell(\ell+1) - 2) - 2 \right] \left(\frac{r}{r_x}\right) + \mathcal{O}\left(\frac{r}{r_x}\right)^2. \quad (\text{C7})$$

As expected we therefore recover δV_1 in the long distance limit and have identified the leading order correction to this when $r/r_x \ll 1$. More generally, one therefore finds that $\delta\tilde{V}_i \simeq \delta V_i + \mathcal{O}(r/r_x)$ and large distance modifications like (C5) therefore only induce strongly suppressed corrections on the potential at small $\mathcal{O}(r_x)$ distances and hence on the QNM spectrum.

²⁸ Note that in (4) we show ψ'^2 , while here we add a large- r correction to ψ' . We choose to add the correction to the derivative of ψ rather than to ψ itself because in shift-symmetric theories the derivatives encode the key information. One can, however see the correction in (C5) as coming from

$$\tilde{\psi} = \int \frac{q}{B} \sqrt{1 - \frac{\lambda B}{\lambda + \eta r^2}} dr + q\lambda \frac{1}{n+1} \left(\frac{r}{r_x}\right)^{n+1} \quad (\text{C4})$$

- [1] A. Bakopoulos, C. Charmousis, P. Kanti, N. Lecoer, and T. Nakas, “Black holes with primary scalar hair,” [arXiv:2310.11919](https://arxiv.org/abs/2310.11919) [gr-qc].
- [2] S. Sirera, “ringdown-calculations.” <https://github.com/sergis1/ringdown-calculations>.
- [3] E. Berti, V. Cardoso, and A. O. Starinets, “Quasinormal modes of black holes and black branes,” *Class. Quant. Grav.* **26** (2009) 163001, [arXiv:0905.2975](https://arxiv.org/abs/0905.2975) [gr-qc].
- [4] P. O. Mazur, “Black hole uniqueness theorems,” [arXiv:hep-th/0101012](https://arxiv.org/abs/hep-th/0101012).
- [5] C.-Y. Chen, M. Bouhmadi-López, and P. Chen, “Lessons from black hole quasinormal modes in modified gravity,” *Eur.*

- Phys. J. Plus* **136** (2021) no. 2, 253, [arXiv:2103.01249](#) [gr-qc].
- [6] C. Bambi, “Testing the Kerr black hole hypothesis,” *Mod. Phys. Lett. A* **26** (2011) 2453–2468, [arXiv:1109.4256](#) [gr-qc].
- [7] O. Dreyer, B. J. Kelly, B. Krishnan, L. S. Finn, D. Garrison, and R. Lopez-Aleman, “Black hole spectroscopy: Testing general relativity through gravitational wave observations,” *Class. Quant. Grav.* **21** (2004) 787–804, [arXiv:gr-qc/0309007](#).
- [8] S. Sirera and J. Noller, “Testing the speed of gravity with black hole ringdowns,” *Phys. Rev. D* **107** (2023) no. 12, 124054, [arXiv:2301.10272](#) [gr-qc].
- [9] J. Bamber, J. C. Aurrekoetxea, K. Clough, and P. G. Ferreira, “Black hole merger simulations in wave dark matter environments,” [arXiv:2210.09254](#) [gr-qc].
- [10] K. J. Taylor and A. Ritz, “Ringdown signatures of Kerr black holes immersed in a magnetic field,” [arXiv:2406.09314](#) [gr-qc].
- [11] O. J. Tattersall and P. G. Ferreira, “Forecasts for Low Spin Black Hole Spectroscopy in Horndeski Gravity,” *Phys. Rev. D* **99** (2019) no. 10, 104082, [arXiv:1904.05112](#) [gr-qc].
- [12] O. J. Tattersall and P. G. Ferreira, “Quasinormal modes of black holes in Horndeski gravity,” *Phys. Rev. D* **97** (2018) no. 10, 104047, [arXiv:1804.08950](#) [gr-qc].
- [13] C. Pitte, Q. Baghi, M. Besançon, and A. Petiteau, “Exploring the no-hair theorem with LISA,” [arXiv:2406.14552](#) [gr-qc].
- [14] E. Berti, V. Cardoso, and C. M. Will, “On gravitational-wave spectroscopy of massive black holes with the space interferometer LISA,” *Phys. Rev. D* **73** (2006) 064030, [arXiv:gr-qc/0512160](#).
- [15] V. Cardoso and P. Pani, “Testing the nature of dark compact objects: a status report,” *Living Rev. Rel.* **22** (2019) no. 1, 4, [arXiv:1904.05363](#) [gr-qc].
- [16] G. Carullo, W. Del Pozzo, and J. Veitch, “Observational Black Hole Spectroscopy: A time-domain multimode analysis of GW150914,” *Phys. Rev. D* **99** (2019) no. 12, 123029, [arXiv:1902.07527](#) [gr-qc]. [Erratum: *Phys.Rev.D* 100, 089903 (2019)].
- [17] J. Meidam, M. Agathos, C. Van Den Broeck, J. Veitch, and B. S. Sathyaprakash, “Testing the no-hair theorem with black hole ringdowns using TIGER,” *Phys. Rev. D* **90** (2014) no. 6, 064009, [arXiv:1406.3201](#) [gr-qc].
- [18] R. Brito, A. Buonanno, and V. Raymond, “Black-hole Spectroscopy by Making Full Use of Gravitational-Wave Modeling,” *Phys. Rev. D* **98** (2018) no. 8, 084038, [arXiv:1805.00293](#) [gr-qc].
- [19] V. Cardoso, M. Kimura, A. Maselli, E. Berti, C. F. B. Macedo, and R. McManus, “Parametrized black hole quasinormal ringdown: Decoupled equations for nonrotating black holes,” *Phys. Rev. D* **99** (2019) no. 10, 104077, [arXiv:1901.01265](#) [gr-qc].
- [20] M. V. S. Saketh and E. Maggio, “Quasinormal modes of slowly-spinning horizonless compact objects,” [arXiv:2406.10070](#) [gr-qc].
- [21] S. Mukohyama, K. Takahashi, K. Tomikawa, and V. Yingcharoenrat, “Quasinormal modes from EFT of black hole perturbations with timelike scalar profile,” *JCAP* **07** (2023) 050, [arXiv:2304.14304](#) [gr-qc].
- [22] L. Pierini and L. Gualtieri, “Quasi-normal modes of rotating black holes in Einstein-dilaton Gauss-Bonnet gravity: the first order in rotation,” *Phys. Rev. D* **103** (2021) 124017, [arXiv:2103.09870](#) [gr-qc].
- [23] P. Wagle, N. Yunes, and H. O. Silva, “Quasinormal modes of slowly-rotating black holes in dynamical Chern-Simons gravity,” *Phys. Rev. D* **105** (2022) no. 12, 124003, [arXiv:2103.09913](#) [gr-qc].
- [24] R. Brito and C. Pacilio, “Quasinormal modes of weakly charged Einstein-Maxwell-dilaton black holes,” *Phys. Rev. D* **98** (2018) no. 10, 104042, [arXiv:1807.09081](#) [gr-qc].
- [25] G. W. Horndeski, “Second-order scalar-tensor field equations in a four-dimensional space,” *Int. J. Theor. Phys.* **10** (1974) 363–384.
- [26] C. Deffayet, X. Gao, D. A. Steer, and G. Zahariade, “From k-essence to generalised Galileons,” *Phys. Rev. D* **84** (2011) 064039, [arXiv:1103.3260](#) [hep-th].
- [27] T. Anson, E. Babichev, C. Charmousis, and M. Hassaine, “Disforming the Kerr metric,” *JHEP* **01** (2021) 018, [arXiv:2006.06461](#) [gr-qc].
- [28] E. Babichev, C. Charmousis, and N. Lecoeur, “Rotating black holes embedded in a cosmological background for scalar-tensor theories,” *JCAP* **08** (2023) 022, [arXiv:2305.17129](#) [gr-qc].
- [29] E. Babichev and C. Charmousis, “Dressing a black hole with a time-dependent Galileon,” *JHEP* **08** (2014) 106, [arXiv:1312.3204](#) [gr-qc].
- [30] T. Kobayashi and N. Tanahashi, “Exact black hole solutions in shift symmetric scalar-tensor theories,” *PTEP* **2014** (2014) 073E02, [arXiv:1403.4364](#) [gr-qc].
- [31] E. Babichev and G. Esposito-Farèse, “Time-Dependent Spherically Symmetric Covariant Galileons,” *Phys. Rev. D* **87** (2013) 044032, [arXiv:1212.1394](#) [gr-qc].
- [32] E. Babichev, C. Charmousis, A. Lehébel, and T. Moskalets, “Black holes in a cubic Galileon universe,” *JCAP* **09** (2016) 011, [arXiv:1605.07438](#) [gr-qc].
- [33] E. Babichev, C. Charmousis, and A. Lehébel, “Asymptotically flat black holes in Horndeski theory and beyond,” *JCAP* **04** (2017) 027, [arXiv:1702.01938](#) [gr-qc].
- [34] E. Babichev and G. Esposito-Farèse, “Cosmological self-tuning and local solutions in generalized Horndeski theories,” *Phys. Rev. D* **95** (2017) no. 2, 024020, [arXiv:1609.09798](#) [gr-qc].
- [35] J. Ben Achour and H. Liu, “Hairy Schwarzschild-(A)dS black hole solutions in degenerate higher order scalar-tensor theories beyond shift symmetry,” *Phys. Rev. D* **99** (2019) no. 6, 064042, [arXiv:1811.05369](#) [gr-qc].
- [36] H. Motohashi and M. Minamitsuji, “Exact black hole solutions in shift-symmetric quadratic degenerate higher-order scalar-tensor theories,” *Phys. Rev. D* **99** (2019) no. 6, 064040, [arXiv:1901.04658](#) [gr-qc].
- [37] K. Takahashi and H. Motohashi, “General Relativity solutions with stealth scalar hair in quadratic higher-order scalar-tensor theories,” *JCAP* **06** (2020) 034, [arXiv:2004.03883](#) [gr-qc].
- [38] K. Takahashi and H. Motohashi, “Black hole perturbations in DHOST theories: master variables, gradient instability, and strong coupling,” *JCAP* **08** (2021) 013, [arXiv:2106.07128](#) [gr-qc].
- [39] E. Babichev, C. Charmousis, and A. Lehébel, “Black holes and stars in Horndeski theory,” *Class. Quant. Grav.* **33** (2016) no. 15, 154002, [arXiv:1604.06402](#) [gr-qc].
- [40] T. Kobayashi, M. Yamaguchi, and J. Yokoyama, “Generalized G-inflation: Inflation with the most general second-order field equations,” *Prog. Theor. Phys.* **126** (2011)

- 511–529, [arXiv:1105.5723 \[hep-th\]](#).
- [41] D. Langlois and K. Noui, “Degenerate higher derivative theories beyond Horndeski: evading the Ostrogradski instability,” *JCAP* **1602** (2016) no. 02, 034, [arXiv:1510.06930 \[gr-qc\]](#).
- [42] M. Crisostomi, K. Koyama, and G. Tasinato, “Extended Scalar-Tensor Theories of Gravity,” *JCAP* **1604** (2016) no. 04, 044, [arXiv:1602.03119 \[hep-th\]](#).
- [43] J. Ben Achour *et al.*, “Degenerate higher order scalar-tensor theories beyond Horndeski up to cubic order,” [arXiv:1608.08135 \[hep-th\]](#).
- [44] K. Takahashi and T. Kobayashi, “Extended mimetic gravity: Hamiltonian analysis and gradient instabilities,” *JCAP* **11** (2017) 038, [arXiv:1708.02951 \[gr-qc\]](#).
- [45] D. Langlois, M. Mancarella, K. Noui, and F. Vernizzi, “Mimetic gravity as DHOST theories,” *JCAP* **02** (2019) 036, [arXiv:1802.03394 \[gr-qc\]](#).
- [46] S. Hawking, “Black holes in the brans-dicke,” *Communications in Mathematical Physics* **25** (1972) no. 2, 167–171.
- [47] T. P. Sotiriou and V. Faraoni, “Black holes in scalar-tensor gravity,” *Phys. Rev. Lett.* **108** (2012) 081103, <https://link.aps.org/doi/10.1103/PhysRevLett.108.081103>.
- [48] L. Hui and A. Nicolis, “No-hair theorem for the galileon,” *Phys. Rev. Lett.* **110** (2013) 241104, <https://link.aps.org/doi/10.1103/PhysRevLett.110.241104>.
- [49] T. P. Sotiriou and S.-Y. Zhou, “Black hole hair in generalized scalar-tensor gravity,” *Phys. Rev. Lett.* **112** (2014) 251102, [arXiv:1312.3622 \[gr-qc\]](#).
- [50] H. Motohashi and M. Minamitsuji, “General Relativity solutions in modified gravity,” *Phys. Lett. B* **781** (2018) 728–734, [arXiv:1804.01731 \[gr-qc\]](#).
- [51] T. Kobayashi, H. Motohashi, and T. Suyama, “Black hole perturbation in the most general scalar-tensor theory with second-order field equations II: the even-parity sector,” *Phys. Rev. D* **89** (2014) no. 8, 084042, [arXiv:1402.6740 \[gr-qc\]](#).
- [52] O. J. Tattersall, P. G. Ferreira, and M. Lagos, “General theories of linear gravitational perturbations to a Schwarzschild Black Hole,” *Phys. Rev. D* **97** (2018) no. 4, 044021, [arXiv:1711.01992 \[gr-qc\]](#).
- [53] G. Franciolini, L. Hui, R. Penco, L. Santoni, and E. Trincherini, “Effective Field Theory of Black Hole Quasinormal Modes in Scalar-Tensor Theories,” *JHEP* **02** (2019) 127, [arXiv:1810.07706 \[hep-th\]](#).
- [54] S. Datta and S. Bose, “Quasi-normal Modes of Static Spherically Symmetric Black Holes in $f(R)$ Theory,” *Eur. Phys. J. C* **80** (2020) no. 1, 14, [arXiv:1904.01519 \[gr-qc\]](#).
- [55] J. Khoury, M. Trodden, and S. S. C. Wong, “Existence and instability of hairy black holes in shift-symmetric Horndeski theories,” *JCAP* **11** (2020) 044, [arXiv:2007.01320 \[astro-ph.CO\]](#).
- [56] R. C. Bernardo and I. Vega, “Stealth black hole perturbations in kinetic gravity braiding,” *J. Math. Phys.* **62** (2021) no. 7, 072501, [arXiv:2007.06006 \[gr-qc\]](#).
- [57] D. Langlois, K. Noui, and H. Roussille, “Linear perturbations of Einstein-Gauss-Bonnet black holes,” *JCAP* **09** (2022) 019, [arXiv:2204.04107 \[gr-qc\]](#).
- [58] M. Minamitsuji, K. Takahashi, and S. Tsujikawa, “Linear stability of black holes in shift-symmetric Horndeski theories with a time-independent scalar field,” *Phys. Rev. D* **105** (2022) no. 10, 104001, [arXiv:2201.09687 \[gr-qc\]](#).
- [59] L. Hui, A. Podo, L. Santoni, and E. Trincherini, “Effective Field Theory for the perturbations of a slowly rotating black hole,” *JHEP* **12** (2021) 183, [arXiv:2111.02072 \[hep-th\]](#).
- [60] C. de Rham and J. Zhang, “Perturbations of stealth black holes in degenerate higher-order scalar-tensor theories,” *Phys. Rev. D* **100** (2019) no. 12, 124023, [arXiv:1907.00699 \[hep-th\]](#).
- [61] D. Langlois, K. Noui, and H. Roussille, “Black hole perturbations in modified gravity,” *Phys. Rev. D* **104** (2021) no. 12, 124044, [arXiv:2103.14750 \[gr-qc\]](#).
- [62] K. Glampedakis and H. O. Silva, “Eikonal quasinormal modes of black holes beyond General Relativity,” *Phys. Rev. D* **100** (2019) no. 4, 044040, [arXiv:1906.05455 \[gr-qc\]](#).
- [63] C.-Y. Chen and S. Park, “Black hole quasinormal modes and isospectrality in Deser-Woodard nonlocal gravity,” *Phys. Rev. D* **103** (2021) no. 6, 064029, [arXiv:2101.06600 \[gr-qc\]](#).
- [64] P. A. Cano, K. Fransen, T. Hertog, and S. Maenaut, “Quasinormal modes of rotating black holes in higher-derivative gravity,” *Phys. Rev. D* **108** (2023) no. 12, 124032, [arXiv:2307.07431 \[gr-qc\]](#).
- [65] M. Minamitsuji and H. Motohashi, “Stealth Schwarzschild solution in shift symmetry breaking theories,” *Phys. Rev. D* **98** (2018) no. 8, 084027, [arXiv:1809.06611 \[gr-qc\]](#).
- [66] C. Charmousis, M. Crisostomi, R. Gregory, and N. Stergioulas, “Rotating Black Holes in Higher Order Gravity,” *Phys. Rev. D* **100** (2019) no. 8, 084020, [arXiv:1903.05519 \[hep-th\]](#).
- [67] S. Mukohyama and V. Yingcharoenrat, “Effective field theory of black hole perturbations with timelike scalar profile: formulation,” *JCAP* **09** (2022) 010, [arXiv:2204.00228 \[hep-th\]](#).
- [68] J. Khoury, T. Noumi, M. Trodden, and S. S. C. Wong, “Stability of hairy black holes in shift-symmetric scalar-tensor theories via the effective field theory approach,” *JCAP* **04** (2023) 035, [arXiv:2208.02823 \[hep-th\]](#).
- [69] S. Mukohyama, K. Takahashi, and V. Yingcharoenrat, “Generalized Regge-Wheeler equation from Effective Field Theory of black hole perturbations with a timelike scalar profile,” *JCAP* **10** (2022) 050, [arXiv:2208.02943 \[gr-qc\]](#).
- [70] R. A. Konoplya, “Quasinormal modes and grey-body factors of regular black holes with a scalar hair from the Effective Field Theory,” *JCAP* **07** (2023) 001, [arXiv:2305.09187 \[gr-qc\]](#).
- [71] C. G. A. Barura, H. Kobayashi, S. Mukohyama, N. Oshita, K. Takahashi, and V. Yingcharoenrat, “Tidal Love Numbers from EFT of Black Hole Perturbations with Timelike Scalar Profile,” [arXiv:2405.10813 \[gr-qc\]](#).
- [72] H. Motohashi and S. Mukohyama, “Weakly-coupled stealth solution in scordatura degenerate theory,” *JCAP* **01** (2020) 030, [arXiv:1912.00378 \[gr-qc\]](#).
- [73] A. De Felice, S. Mukohyama, and K. Takahashi, “Avoidance of Strong Coupling in General Relativity Solutions with a Timelike Scalar Profile in a Class of Ghost-Free Scalar-Tensor Theories,” *Phys. Rev. Lett.* **129** (2022) no. 3, 031103, [arXiv:2204.02032 \[gr-qc\]](#).
- [74] A. Iyonaga, K. Takahashi, and T. Kobayashi, “Extended Cuscuton: Formulation,” *JCAP* **12** (2018) 002, [arXiv:1809.10935 \[gr-qc\]](#).
- [75] N. Afshordi, D. J. H. Chung, and G. Geshnizjani, “Cuscuton: A Causal Field Theory with an Infinite Speed of Sound,”

- Phys. Rev. D* **75** (2007) 083513, [arXiv:hep-th/0609150](https://arxiv.org/abs/hep-th/0609150).
- [76] N. Afshordi, D. J. H. Chung, M. Doran, and G. Geshnizjani, “Cuscuton Cosmology: Dark Energy meets Modified Gravity,” *Phys. Rev. D* **75** (2007) 123509, [arXiv:astro-ph/0702002](https://arxiv.org/abs/astro-ph/0702002).
- [77] J. Saito and T. Kobayashi, “Black hole perturbations in spatially covariant gravity with just two tensorial degrees of freedom,” *Phys. Rev. D* **108** (2023) no. 10, 104063, [arXiv:2308.00267](https://arxiv.org/abs/2308.00267) [gr-qc].
- [78] A. Iyonaga, K. Takahashi, and T. Kobayashi, “Extended Cuscuton as Dark Energy,” *JCAP* **07** (2020) 004, [arXiv:2003.01934](https://arxiv.org/abs/2003.01934) [gr-qc].
- [79] D. Brizuela, J. M. Martin-Garcia, and G. A. Mena Marugan, “Second and higher-order perturbations of a spherical spacetime,” *Phys. Rev. D* **74** (2006) 044039, [arXiv:gr-qc/0607025](https://arxiv.org/abs/gr-qc/0607025).
- [80] D. Brizuela, J. M. Martin-Garcia, and G. A. M. Marugan, “High-order gauge-invariant perturbations of a spherical spacetime,” *Phys. Rev. D* **76** (2007) 024004, [arXiv:gr-qc/0703069](https://arxiv.org/abs/gr-qc/0703069).
- [81] D. Brizuela, J. M. Martin-Garcia, and M. Tiglio, “A Complete gauge-invariant formalism for arbitrary second-order perturbations of a Schwarzschild black hole,” *Phys. Rev. D* **80** (2009) 024021, [arXiv:0903.1134](https://arxiv.org/abs/0903.1134) [gr-qc].
- [82] M. Lagos and L. Hui, “Generation and propagation of nonlinear quasi-normal modes of a Schwarzschild black hole,” [arXiv:2208.07379](https://arxiv.org/abs/2208.07379) [gr-qc].
- [83] K. Mitman *et al.*, “Nonlinearities in black hole ringdowns,” [arXiv:2208.07380](https://arxiv.org/abs/2208.07380) [gr-qc].
- [84] M. H.-Y. Cheung *et al.*, “Nonlinear effects in black hole ringdown,” [arXiv:2208.07374](https://arxiv.org/abs/2208.07374) [gr-qc].
- [85] T. Regge and J. A. Wheeler, “Stability of a Schwarzschild singularity,” *Phys. Rev.* **108** (1957) 1063–1069.
- [86] K. Takahashi, H. Motohashi, and M. Minamitsuji, “Linear stability analysis of hairy black holes in quadratic degenerate higher-order scalar-tensor theories: Odd-parity perturbations,” *Phys. Rev. D* **100** (2019) no. 2, 024041, [arXiv:1904.03554](https://arxiv.org/abs/1904.03554) [gr-qc].
- [87] H. Ogawa, T. Kobayashi, and T. Suyama, “Instability of hairy black holes in shift-symmetric Horndeski theories,” *Phys. Rev. D* **93** (2016) no. 6, 064078, [arXiv:1510.07400](https://arxiv.org/abs/1510.07400) [gr-qc].
- [88] K. Nakashi, M. Kimura, H. Motohashi, and K. Takahashi, “Black hole ringdown from physically sensible initial value problem in higher-order scalar-tensor theories,” [arXiv:2310.09839](https://arxiv.org/abs/2310.09839) [gr-qc].
- [89] E. Babichev, C. Charmousis, G. Esposito-Farèse, and A. Lehébel, “Hamiltonian unboundedness vs stability with an application to Horndeski theory,” *Phys. Rev. D* **98** (2018) no. 10, 104050, [arXiv:1803.11444](https://arxiv.org/abs/1803.11444) [gr-qc].
- [90] V. Ferrari and B. Mashhoon, “New approach to the quasinormal modes of a black hole,” *Phys. Rev. D* **30** (1984) 295–304.
- [91] C. J. Goebel, “Comments on the “vibrations” of a Black Hole.,” *ApJ* **172** (1972) L95.
- [92] B. F. Schutz and C. M. Will, “Black hole normal modes - A semianalytic approach,” *ApJ* **291** (1985) L33–L36.
- [93] L. Motl and A. Neitzke, “Asymptotic black hole quasinormal frequencies,” *Adv. Theor. Math. Phys.* **7** (2003) no. 2, 307–330, [arXiv:hep-th/0301173](https://arxiv.org/abs/hep-th/0301173).
- [94] G. T. Horowitz and V. E. Hubeny, “Quasinormal modes of AdS black holes and the approach to thermal equilibrium,” *Phys. Rev. D* **62** (2000) 024027, [arXiv:hep-th/9909056](https://arxiv.org/abs/hep-th/9909056).
- [95] E. Berti, V. Cardoso, and P. Pani, “Breit-Wigner resonances and the quasinormal modes of anti-de Sitter black holes,” *Phys. Rev. D* **79** (2009) 101501, [arXiv:0903.5311](https://arxiv.org/abs/0903.5311) [gr-qc].
- [96] E. W. Leaver, “An Analytic representation for the quasinormal modes of Kerr black holes,” *Proc. Roy. Soc. Lond. A* **402** (1985) 285–298.
- [97] V. Cardoso, M. Kimura, A. Maselli, E. Berti, C. F. B. Macedo, and R. McManus, “Parametrized black hole quasinormal ringdown: Decoupled equations for nonrotating black holes,” *Phys. Rev. D* **99** (2019) no. 10, 104077, [arXiv:1901.01265](https://arxiv.org/abs/1901.01265) [gr-qc].
- [98] S. Iyer and C. M. Will, “Black Hole Normal Modes: A WKB Approach. I. Foundations and Application of a Higher Order WKB Analysis of Potential Barrier Scattering,” *Phys. Rev. D* **35** (1987) 3621.
- [99] R. A. Konoplya, “Quasinormal behavior of the d-dimensional Schwarzschild black hole and higher order WKB approach,” *Phys. Rev. D* **68** (2003) 024018, [arXiv:gr-qc/0303052](https://arxiv.org/abs/gr-qc/0303052).
- [100] J. Matyjasek and M. Opala, “Quasinormal modes of black holes. The improved semianalytic approach,” *Phys. Rev. D* **96** (2017) no. 2, 024011, [arXiv:1704.00361](https://arxiv.org/abs/1704.00361) [gr-qc].
- [101] R. A. Konoplya, A. Zhidenko, and A. F. Zinhailo, “Higher order WKB formula for quasinormal modes and grey-body factors: recipes for quick and accurate calculations,” *Class. Quant. Grav.* **36** (2019) 155002, [arXiv:1904.10333](https://arxiv.org/abs/1904.10333) [gr-qc].
- [102] R. McManus, E. Berti, C. F. B. Macedo, M. Kimura, A. Maselli, and V. Cardoso, “Parametrized black hole quasinormal ringdown. II. Coupled equations and quadratic corrections for nonrotating black holes,” *Phys. Rev. D* **100** (2019) no. 4, 044061, [arXiv:1906.05155](https://arxiv.org/abs/1906.05155) [gr-qc].
- [103] M. Kimura, “Note on the parametrized black hole quasinormal ringdown formalism,” *Phys. Rev. D* **101** (2020) no. 6, 064031, [arXiv:2001.09613](https://arxiv.org/abs/2001.09613) [gr-qc].
- [104] N. Franchini and S. H. Völkel, “Parametrized quasinormal mode framework for non-Schwarzschild metrics,” *Phys. Rev. D* **107** (2023) no. 12, 124063, [arXiv:2210.14020](https://arxiv.org/abs/2210.14020) [gr-qc].
- [105] R. A. Konoplya, A. Zhidenko, and A. F. Zinhailo, “Mathematica WKB package.” <https://docs.google.com/document/d/1Qot9n954AhM-euRylcBgPx77devbVjoAiyLwLUqHVmA/preview>.
- [106] E. Berti, V. Cardoso, and C. M. Will, “On gravitational-wave spectroscopy of massive black holes with the space interferometer LISA,” *Phys. Rev. D* **73** (2006) 064030, [arXiv:gr-qc/0512160](https://arxiv.org/abs/gr-qc/0512160).
- [107] L. London, D. Shoemaker, and J. Healy, “Modeling ringdown: Beyond the fundamental quasinormal modes,” *Phys. Rev. D* **90** (2014) no. 12, 124032, [arXiv:1404.3197](https://arxiv.org/abs/1404.3197) [gr-qc]. [Erratum: *Phys.Rev.D* 94, 069902 (2016)].
- [108] E. Berti, V. Cardoso, J. A. Gonzalez, U. Sperhake, M. Hannam, S. Husa, and B. Bruegmann, “Inspiral, merger and ringdown of unequal mass black hole binaries: A Multipolar analysis,” *Phys. Rev. D* **76** (2007) 064034, [arXiv:gr-qc/0703053](https://arxiv.org/abs/gr-qc/0703053).
- [109] E. Berti, J. Cardoso, V. Cardoso, and M. Cavaglia, “Matched-filtering and parameter estimation of ringdown waveforms,” *Phys. Rev. D* **76** (2007) 104044, [arXiv:0707.1202](https://arxiv.org/abs/0707.1202) [gr-qc].

- [110] S. Bhagwat, M. Cabero, C. D. Capano, B. Krishnan, and D. A. Brown, “Detectability of the subdominant mode in a binary black hole ringdown,” *Phys. Rev. D* **102** (2020) no. 2, 024023, [arXiv:1910.13203 \[gr-qc\]](#).
- [111] S. Bhagwat, X. J. Forteza, P. Pani, and V. Ferrari, “Ringdown overtones, black hole spectroscopy, and no-hair theorem tests,” *Phys. Rev. D* **101** (2020) no. 4, 044033, [arXiv:1910.08708 \[gr-qc\]](#).
- [112] I. Kamaretsos, M. Hannam, S. Husa, and B. S. Sathyaprakash, “Black-hole hair loss: learning about binary progenitors from ringdown signals,” *Phys. Rev. D* **85** (2012) 024018, [arXiv:1107.0854 \[gr-qc\]](#).
- [113] V. Baibhav, E. Berti, and V. Cardoso, “LISA parameter estimation and source localization with higher harmonics of the ringdown,” *Phys. Rev. D* **101** (2020) no. 8, 084053, [arXiv:2001.10011 \[gr-qc\]](#).
- [114] **LIGO Scientific, Virgo** Collaboration, B. P. Abbott *et al.*, “Binary Black Hole Population Properties Inferred from the First and Second Observing Runs of Advanced LIGO and Advanced Virgo,” *Astrophys. J. Lett.* **882** (2019) no. 2, L24, [arXiv:1811.12940 \[astro-ph.HE\]](#).
- [115] P. C. Peters, “Gravitational radiation and the motion of two point masses,” *Phys. Rev.* **136** (1964) B1224–B1232. <https://link.aps.org/doi/10.1103/PhysRev.136.B1224>.
- [116] I. Hinder, B. Vaishnav, F. Herrmann, D. M. Shoemaker, and P. Laguna, “Circularization and final spin in eccentric binary-black-hole inspirals,” *Phys. Rev. D* **77** (2008) 081502. <https://link.aps.org/doi/10.1103/PhysRevD.77.081502>.
- [117] T. Kobayashi, H. Motohashi, and T. Suyama, “Black hole perturbation in the most general scalar-tensor theory with second-order field equations I: the odd-parity sector,” *Phys. Rev. D* **85** (2012) 084025, [arXiv:1202.4893 \[gr-qc\]](#). [Erratum: *Phys.Rev.D* 96, 109903 (2017)].
- [118] O. J. Tattersall, “Kerr-(anti-)de Sitter black holes: Perturbations and quasinormal modes in the slow rotation limit,” *Phys. Rev. D* **98** (2018) no. 10, 104013, [arXiv:1808.10758 \[gr-qc\]](#).
- [119] P. Pani, V. Cardoso, L. Gualtieri, E. Berti, and A. Ishibashi, “Perturbations of slowly rotating black holes: massive vector fields in the Kerr metric,” *Phys. Rev. D* **86** (2012) 104017, [arXiv:1209.0773 \[gr-qc\]](#).
- [120] P. PANI, “Advanced methods in black-hole perturbation theory,” *International Journal of Modern Physics A* **28** (2013) no. 22n23, 1340018, <https://doi.org/10.1142/S0217751X13400186>. <https://doi.org/10.1142/S0217751X13400186>.
- [121] P. Pani, E. Berti, and L. Gualtieri, “Scalar, Electromagnetic and Gravitational Perturbations of Kerr-Newman Black Holes in the Slow-Rotation Limit,” *Phys. Rev. D* **88** (2013) 064048, [arXiv:1307.7315 \[gr-qc\]](#).
- [122] R. Brito, V. Cardoso, and P. Pani, “Massive spin-2 fields on black hole spacetimes: Instability of the Schwarzschild and Kerr solutions and bounds on the graviton mass,” *Phys. Rev. D* **88** (2013) no. 2, 023514, [arXiv:1304.6725 \[gr-qc\]](#).
- [123] O. J. Tattersall, “Quasi-Normal Modes of Hairy Scalar Tensor Black Holes: Odd Parity,” *Class. Quant. Grav.* **37** (2020) no. 11, 115007, [arXiv:1911.07593 \[gr-qc\]](#).
- [124] H. Yang, K. Yagi, J. Blackman, L. Lehner, V. Paschalidis, F. Pretorius, and N. Yunes, “Black hole spectroscopy with coherent mode stacking,” *Phys. Rev. Lett.* **118** (2017) no. 16, 161101, [arXiv:1701.05808 \[gr-qc\]](#).
- [125] E. Berti, “Lisa observations of massive black hole mergers: event rates and issues in waveform modelling,” *Class. Quant. Grav.* **23** (2006) S785–S798, [arXiv:astro-ph/0602470](#).
- [126] A. Sesana, F. Haardt, P. Madau, and M. Volonteri, “The gravitational wave signal from massive black hole binaries and its contribution to the LISA data stream,” *Astrophys. J.* **623** (2005) 23–30, [arXiv:astro-ph/0409255](#).
- [127] K. J. Rhook and J. S. B. Wyithe, “Realistic event rates for detection of supermassive black hole coalescence by LISA,” *Mon. Not. Roy. Astron. Soc.* **361** (2005) 1145–1152, [arXiv:astro-ph/0503210](#).
- [128] T. Tanaka and Z. Haiman, “The Assembly of Supermassive Black Holes at High Redshifts,” *Astrophys. J.* **696** (2009) 1798–1822, [arXiv:0807.4702 \[astro-ph\]](#).
- [129] **eLISA** Collaboration, P. A. Seoane *et al.*, “The Gravitational Universe,” [arXiv:1305.5720 \[astro-ph.CO\]](#).
- [130] M. Bonetti, A. Sesana, F. Haardt, E. Barausse, and M. Colpi, “Post-Newtonian evolution of massive black hole triplets in galactic nuclei – IV. Implications for LISA,” *Mon. Not. Roy. Astron. Soc.* **486** (2019) no. 3, 4044–4060, [arXiv:1812.01011 \[astro-ph.GA\]](#).
- [131] A. L. Erickcek, M. Kamionkowski, and A. J. Benson, “Supermassive Black Hole Merger Rates: Uncertainties from Halo Merger Theory,” *Mon. Not. Roy. Astron. Soc.* **371** (2006) 1992–2000, [arXiv:astro-ph/0604281](#).
- [132] **Virgo, LIGO Scientific** Collaboration, B. P. Abbott *et al.*, “Tests of general relativity with GW150914,” *Phys. Rev. Lett.* **116** (2016) no. 22, 221101, [arXiv:1602.03841 \[gr-qc\]](#).
- [133] E. E. Flanagan and S. A. Hughes, “Measuring gravitational waves from binary black hole coalescences: 1. Signal-to-noise for inspiral, merger, and ringdown,” *Phys. Rev. D* **57** (1998) 4535–4565, [arXiv:gr-qc/9701039](#).
- [134] H. Nakano, R. Fujita, S. Isoyama, and N. Sago, “Scope out multiband gravitational-wave observations of GW190521-like binary black holes with space gravitational wave antenna B-DECIGO,” *Universe* **7** (2021) no. 3, 53, [arXiv:2101.06402 \[gr-qc\]](#).
- [135] M. Maggiore *et al.*, “Science Case for the Einstein Telescope,” *JCAP* **03** (2020) 050, [arXiv:1912.02622 \[astro-ph.CO\]](#).
- [136] M. Evans *et al.*, “A Horizon Study for Cosmic Explorer: Science, Observatories, and Community,” [arXiv:2109.09882 \[astro-ph.IM\]](#).
- [137] E. D. Hall, “Cosmic Explorer: A Next-Generation Ground-Based Gravitational-Wave Observatory,” *Galaxies* **10** (2022) no. 4, 90.
- [138] T. Nakamura *et al.*, “Pre-DECIGO can get the smoking gun to decide the astrophysical or cosmological origin of GW150914-like binary black holes,” *PTEP* **2016** (2016) no. 9, 093E01, [arXiv:1607.00897 \[astro-ph.HE\]](#).
- [139] R. Nair and T. Tanaka, “Synergy between ground and space based gravitational wave detectors. Part II: Localisation,” *JCAP* **08** (2018) 033, [arXiv:1805.08070 \[gr-qc\]](#). [Erratum: *JCAP* 11, E01 (2018)].
- [140] **AEDGE** Collaboration, Y. A. El-Neaj *et al.*, “AEDGE: Atomic Experiment for Dark Matter and Gravity Exploration in Space,” *EPJ Quant. Technol.* **7** (2020) 6, [arXiv:1908.00802 \[gr-qc\]](#).
- [141] C. Zhang, Y. Gong, and C. Zhang, “Parameter estimation for space-based gravitational wave detectors with ringdown signals,” *Phys. Rev. D* **104** (2021) no. 8, 083038,

- [arXiv:2105.11279](https://arxiv.org/abs/2105.11279) [gr-qc].
- [142] V. Baibhav *et al.*, “Probing the nature of black holes: Deep in the mHz gravitational-wave sky,” *Exper. Astron.* **51** (2021) no. 3, 1385–1416, [arXiv:1908.11390](https://arxiv.org/abs/1908.11390) [astro-ph.HE].
- [143] **LDC Working Group** Collaboration, Q. Baghi, “The LISA Data Challenges,” in *56th Rencontres de Moriond on Gravitation*. 4, 2022. [arXiv:2204.12142](https://arxiv.org/abs/2204.12142) [gr-qc].
- [144] **Mock LISA Data Challenge Task Force** Collaboration, S. Babak *et al.*, “The Mock LISA Data Challenges: From Challenge 3 to Challenge 4,” *Class. Quant. Grav.* **27** (2010) 084009, [arXiv:0912.0548](https://arxiv.org/abs/0912.0548) [gr-qc].
- [145] J. M. “Martín-García, “xAct.” <http://www.xact.es/>.
- [146] B. Hu, M. Raveri, N. Frusciante, and A. Silvestri, “Effective Field Theory of Cosmic Acceleration: an implementation in CAMB,” *Phys. Rev. D* **89** (2014) no. 10, 103530, [arXiv:1312.5742](https://arxiv.org/abs/1312.5742) [astro-ph.CO].
- [147] A. Lehébel, *Compact astrophysical objects in modified gravity*. PhD thesis, Orsay, 2018. [arXiv:1810.04434](https://arxiv.org/abs/1810.04434) [gr-qc].
- [148] N. Lecoœur, “Exact black hole solutions in scalar-tensor theories,” other thesis, 6, 2024.
- [149] T. P. Sotiriou and S.-Y. Zhou, “Black hole hair in generalized scalar-tensor gravity: An explicit example,” *Phys. Rev. D* **90** (2014) 124063, [arXiv:1408.1698](https://arxiv.org/abs/1408.1698) [gr-qc].
- [150] M. Saravani and T. P. Sotiriou, “Classification of shift-symmetric Horndeski theories and hairy black holes,” *Phys. Rev. D* **99** (2019) no. 12, 124004, [arXiv:1903.02055](https://arxiv.org/abs/1903.02055) [gr-qc].
- [151] A. Barreira, B. Li, A. Sanchez, C. M. Baugh, and S. Pascoli, “Parameter space in Galileon gravity models,” *Phys. Rev. D* **87** (2013) 103511, [arXiv:1302.6241](https://arxiv.org/abs/1302.6241) [astro-ph.CO].
- [152] C. Charmousis, E. J. Copeland, A. Padilla, and P. M. Saffin, “General second order scalar-tensor theory, self tuning, and the Fab Four,” *Phys. Rev. Lett.* **108** (2012) 051101, [arXiv:1106.2000](https://arxiv.org/abs/1106.2000) [hep-th].
- [153] K. Takahashi and T. Suyama, “Linear perturbation analysis of hairy black holes in shift-symmetric Horndeski theories: Odd-parity perturbations,” *Phys. Rev. D* **95** (2017) no. 2, 024034, [arXiv:1610.00432](https://arxiv.org/abs/1610.00432) [gr-qc].
- [154] M. Minamitsuji and J. Edholm, “Black holes with a nonconstant kinetic term in degenerate higher-order scalar tensor theories,” *Phys. Rev. D* **101** (2020) no. 4, 044034, [arXiv:1912.01744](https://arxiv.org/abs/1912.01744) [gr-qc].
- [155] A. Zhidenko, “Quasinormal modes of Schwarzschild de Sitter black holes,” *Class. Quant. Grav.* **21** (2004) 273–280, [arXiv:gr-qc/0307012](https://arxiv.org/abs/gr-qc/0307012).
- [156] E. Barausse, V. Cardoso, and P. Pani, “Can environmental effects spoil precision gravitational-wave astrophysics?,” *Phys. Rev. D* **89** (2014) no. 10, 104059, [arXiv:1404.7149](https://arxiv.org/abs/1404.7149) [gr-qc].